

Max Planck
Society



Max Planck
Institute



Image processing workflows for Tomography

Winter School on Structural Cell Biology

Julio Ortiz

Wolfgang Baumeister

MPI of Biochemistry

Dept. of Structural Molecular Biology

Martinsried, Germany

Summary/Outlook

Sample Preparation



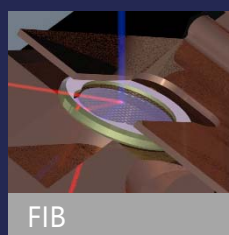
In vitro



In situ



Plunge freezing
-180 °C



FIB

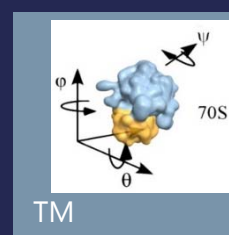
Electron Cryotomography



Single-axis tilt



Dual-axis tilt



TM

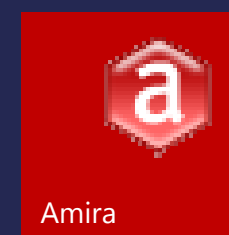
Software



Matlab
toolbox



PyTom



Amira



Chimera



3ds Max



Adobe CS6

Instrumentation



FEI Quanta 3D



FEI Titan Krios



Direct Electron
Detectors



Phase Plate



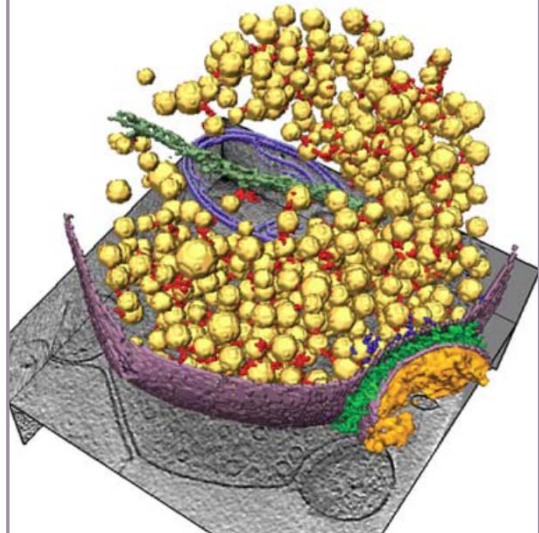
CET combines the power of 3-D imaging
with a close-to-life preservation of cellular
structures and a **allows to study**
macromolecular structures *in situ*.



Cryo-electron tomography (CET)

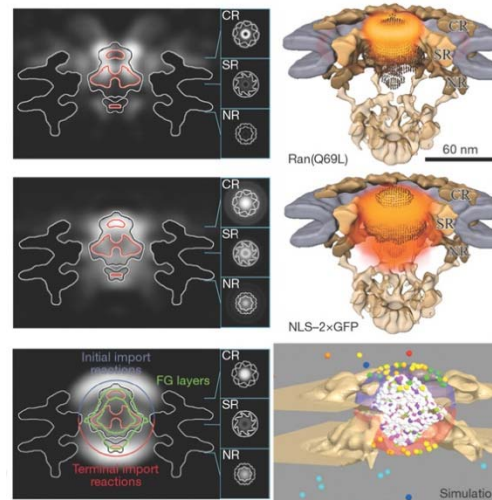
Low-level Techniques for Data Analysis in Tomography

Segmentation



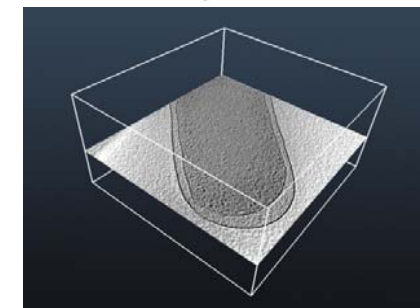
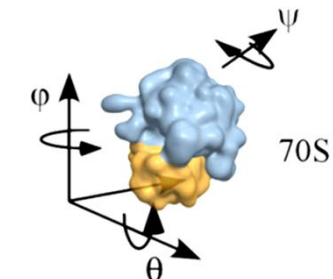
Presynaptic vesicles
Fernández-Busnadio, R. et al.,
J. Cell. Biol. (2010)

Electron-dense labeling



NPC substrate localization
Beck, M., et al., *Nature* (2007)

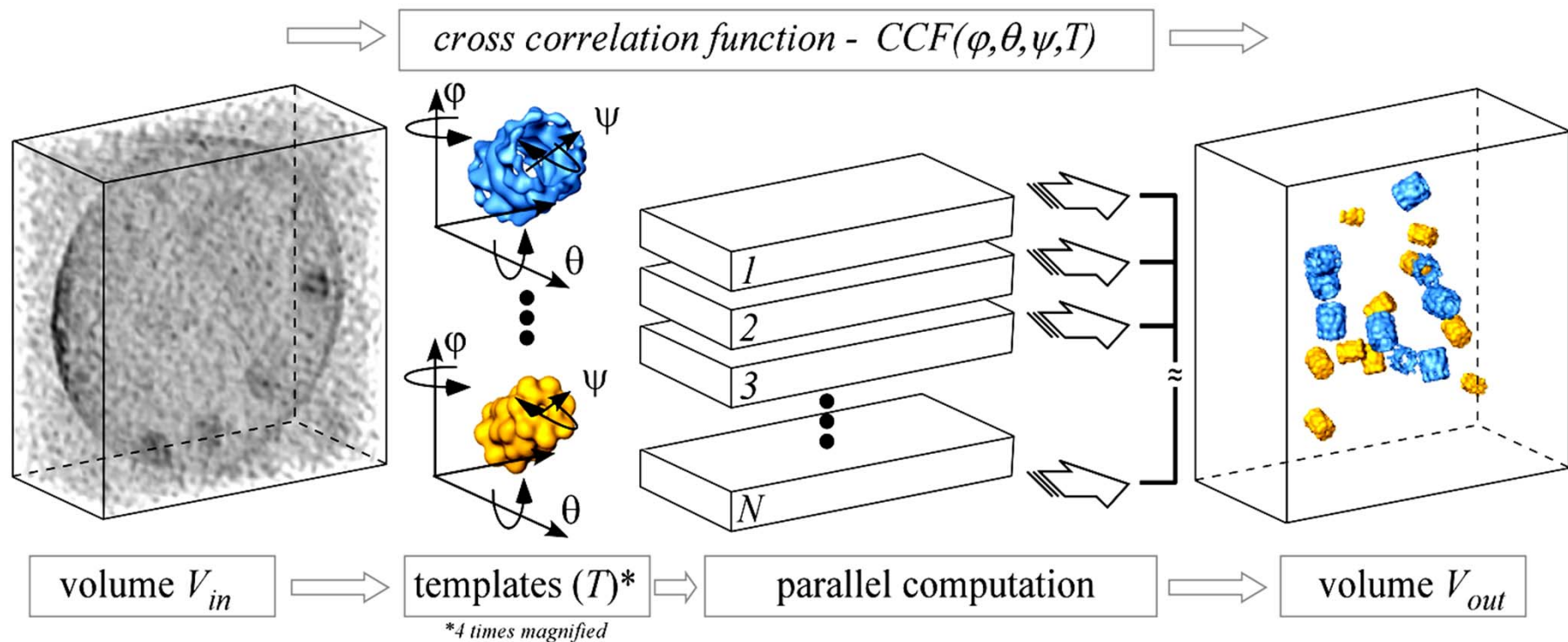
Template Matching



Boehm, J. et al. *Proc Natl Acad Sci U S A.* (2000)



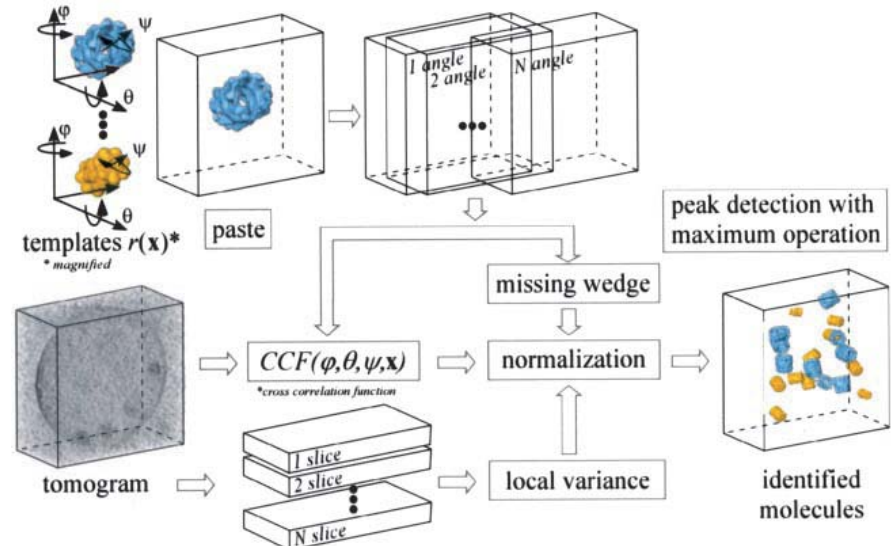
Detection and identification strategy



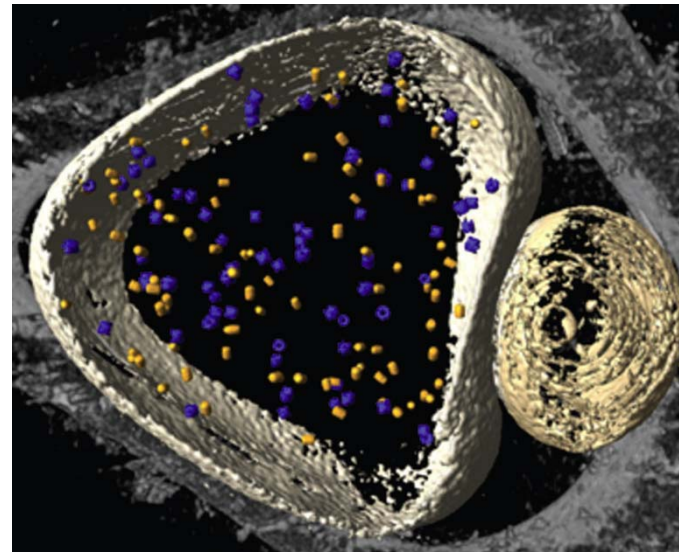
A.S. Frangakis, J. Böhm, F. Förster, S. Nickell, D. Nicastro, D. Typke, R. Hegerl, W. Baumeister:
Proc Natl Acad Sci USA 99 (2002) 14153-14158



Identification of macromolecular complexes in cryo-electron tomograms of phantom cells



Schematic flow diagram showing the detection and identification strategy

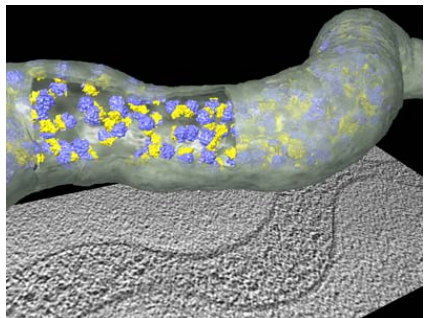


Thermosomes and 20S proteasomes encapsulated in liposomes

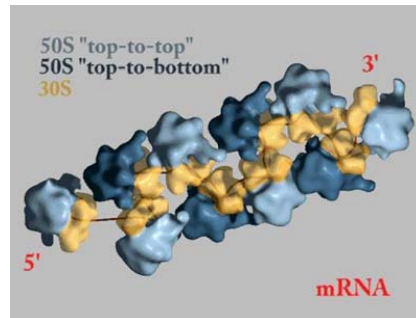
Frangakis, A. et al., *PNAS* (2002)



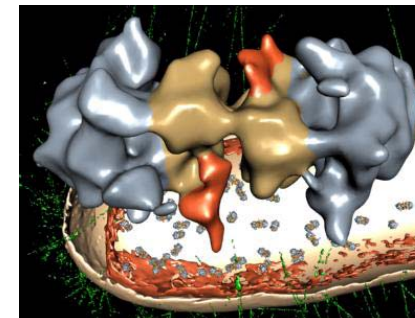
2002-2012: Template Matching Achievements



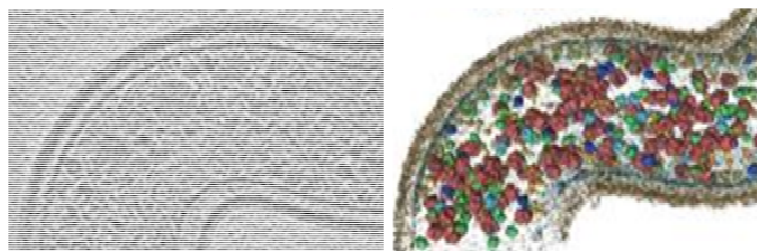
Spiroplasma
Ortiz, J., et al. *J. Struct. Biol.* (2006)



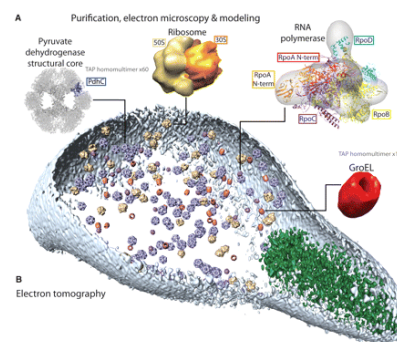
*Polysomes *in vitro**
Brandt, F., et al. *Cell.* (2009)



*Hibernating ribosomes (*in vitro* & *in vivo*)*
Ortiz, J., et al. *J. Cell. Biol.* (2010)



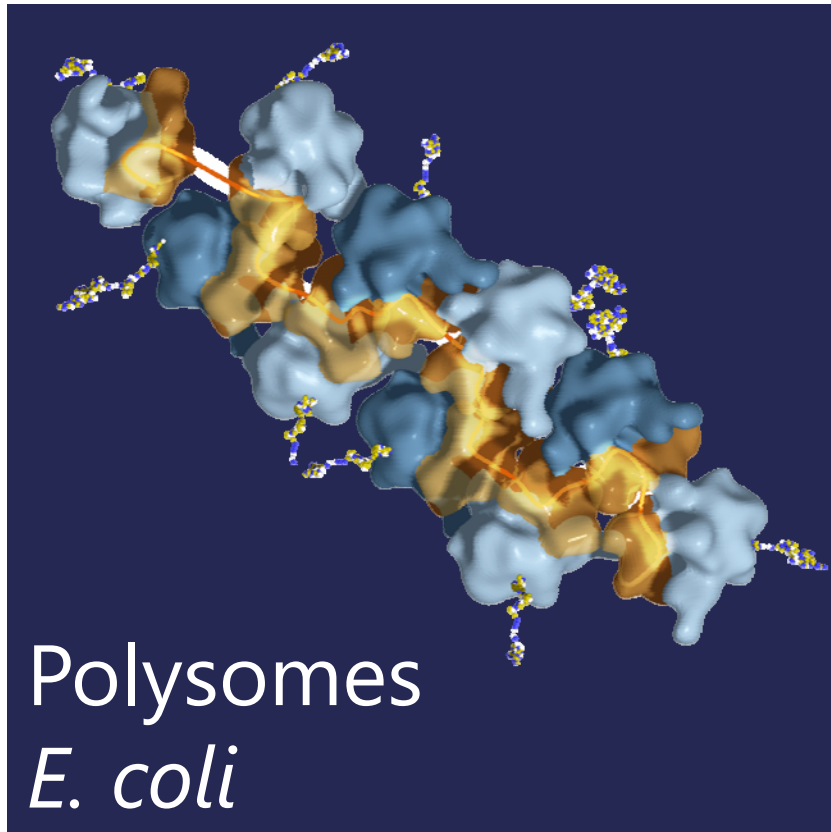
Visual Proteomics - *Leptospira*
Beck, M., et al. *Nat. Methods* (2009)



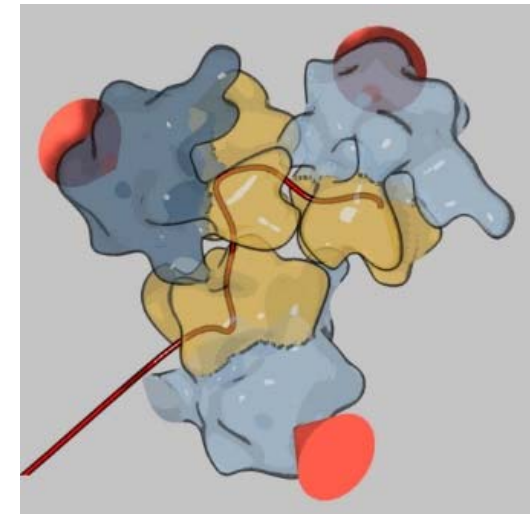
Visual Proteomics - *Mycoplasma*
Kuerner, S., et al. *Science* (2009)



Polysomes *in situ*



E. coli

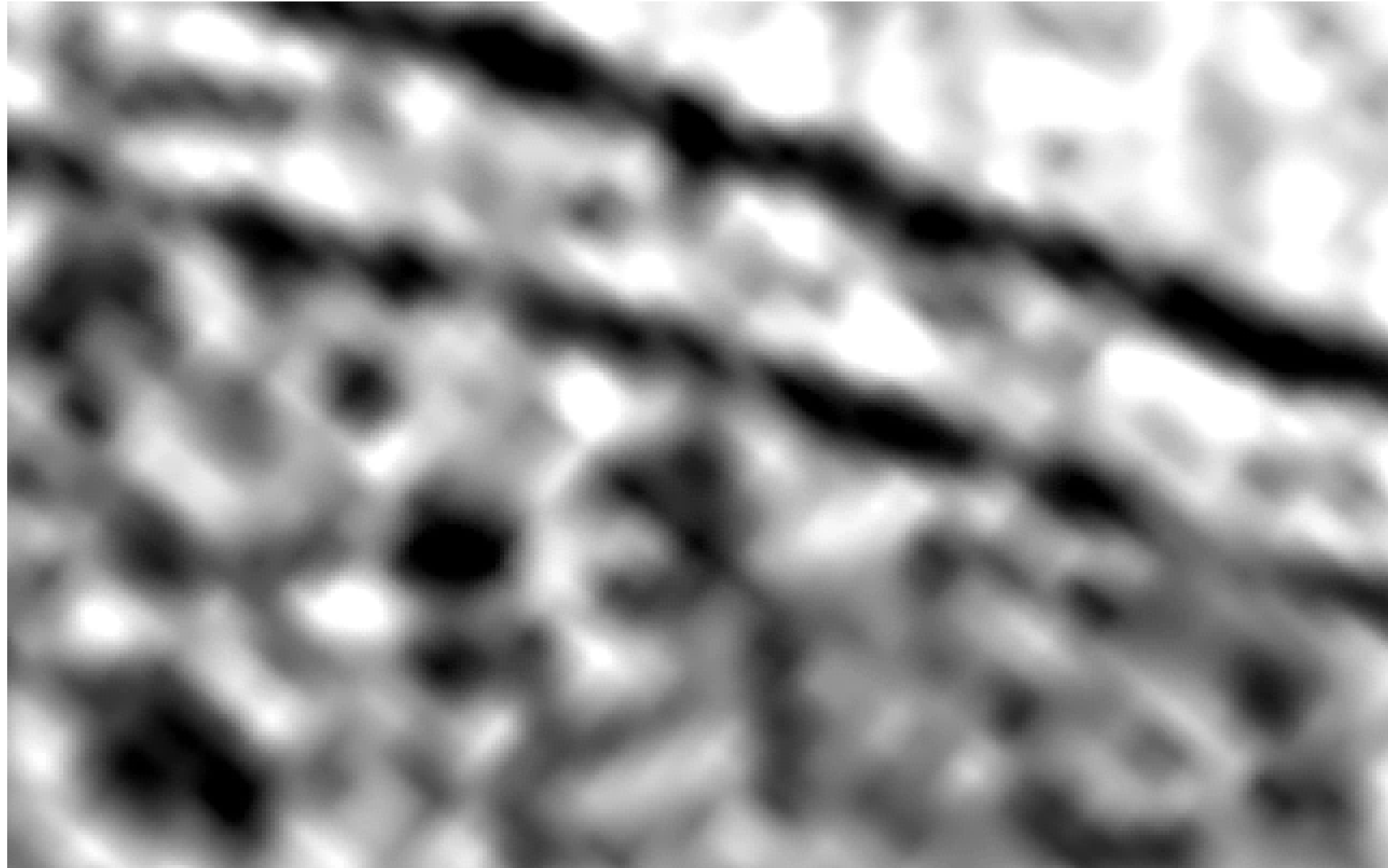


Aim:

To detect ribosomal supramolecular arrangements in the cytoplasm of fast growing *E. coli* cells.

Brandt, F. et al. *Cell*. 2009 **23**:261-71





Tomogram of thin whole *E. coli* cell
(slow growing cell; CCD- camera)

Cryo-ultramicrotomy- Diamond Knife



PATENT SPECIFICATION

799,498

Date of Application and filing Complete Specification: Sept. 2, 1955.

No. 10682/57.

Application made in Sweden on Sept. 4, 1954.

(Divided out of No. 799,497).

Complete Specification Published: Aug. 6, 1958.

Index at acceptance:—Class 60, D1(D4X: H17), D2(A15: A20: K).

International Classification:—B24b.

COMPLETE SPECIFICATION

Improvements in or relating to a method of Polishing a Cutting Edge of a Diamond for a Cutting Tool

I, HUMBERTO FERNÁNDEZ-MORIM, of Instituto Venezolano de Neurología e Investigaciones Cerebrales, Ministerio de Sanidad, Caracas, Venezuela, a National of Venezuela, do hereby declare the invention, for which I pray that a patent may be granted to me, and the method by which it is to be performed, to be particularly described in and by the following statement:—

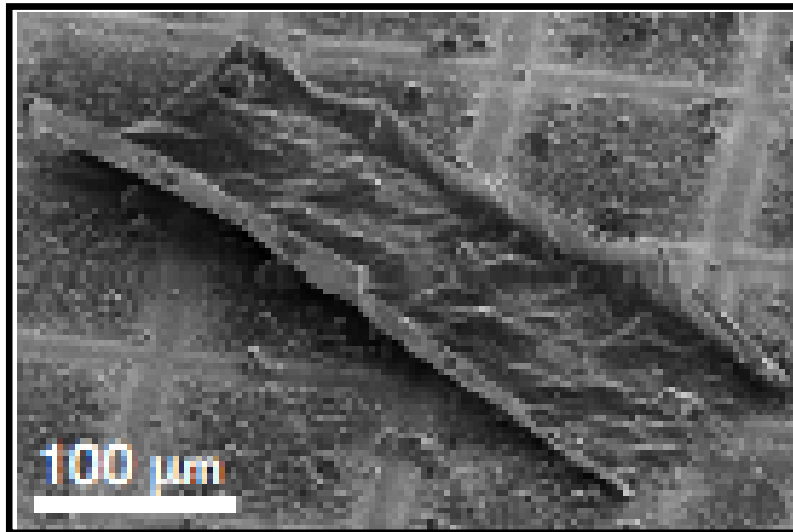
The advantageous effect of the grain size chosen has been found in practice and may perhaps be explained as follows:—

By using a paste comprising diamond powder of a grain size between 0.002 and 0.005 micron, the frictional effects on the diamond being polished are such as to produce a high temperature having a burning-off effect on surface irregularities, rather than a wearing-

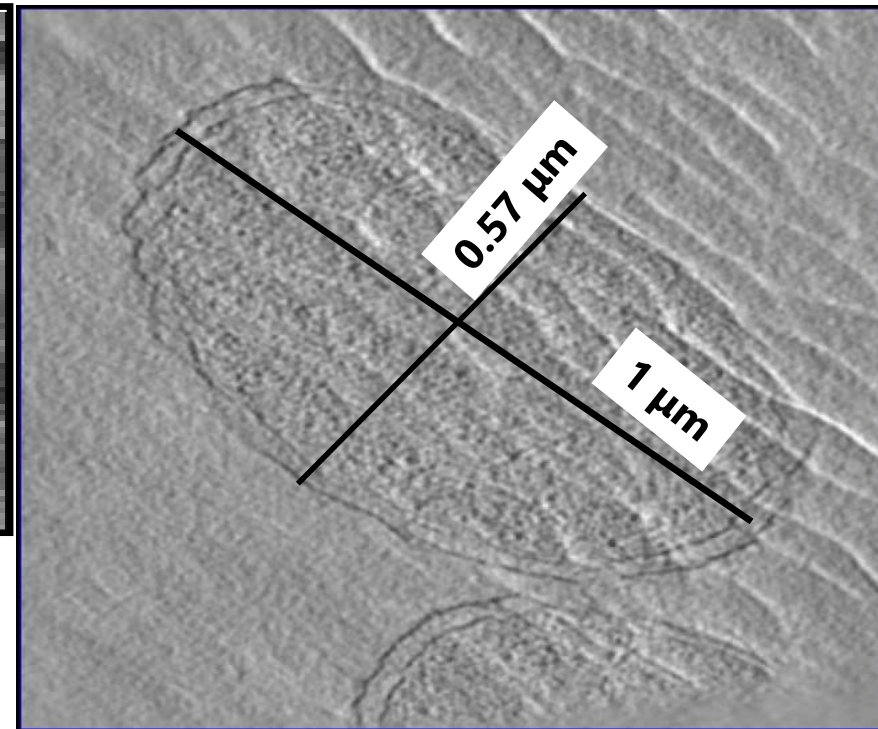


Cryo-ultramicrotomy

Cryo-section



E. coli cell

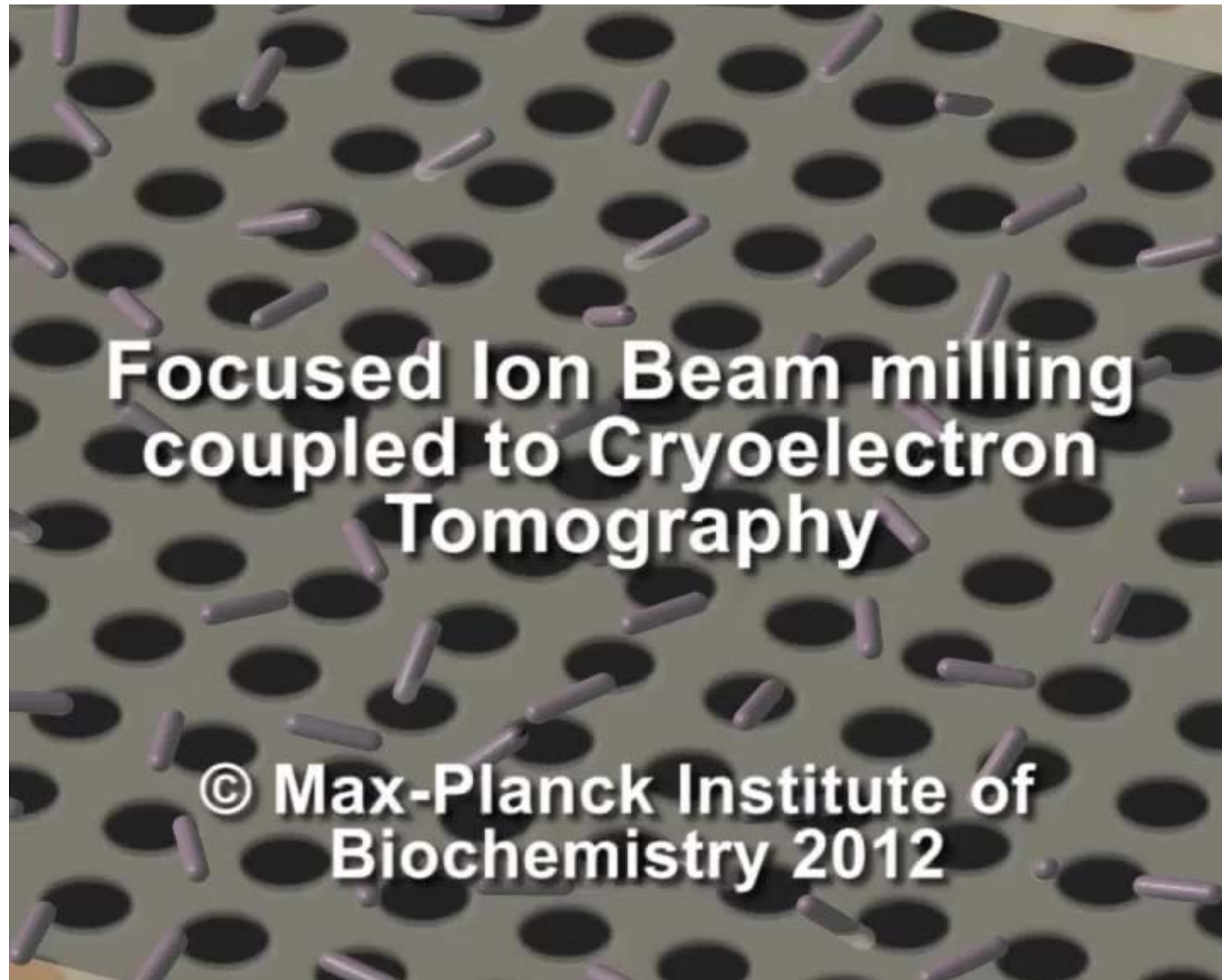


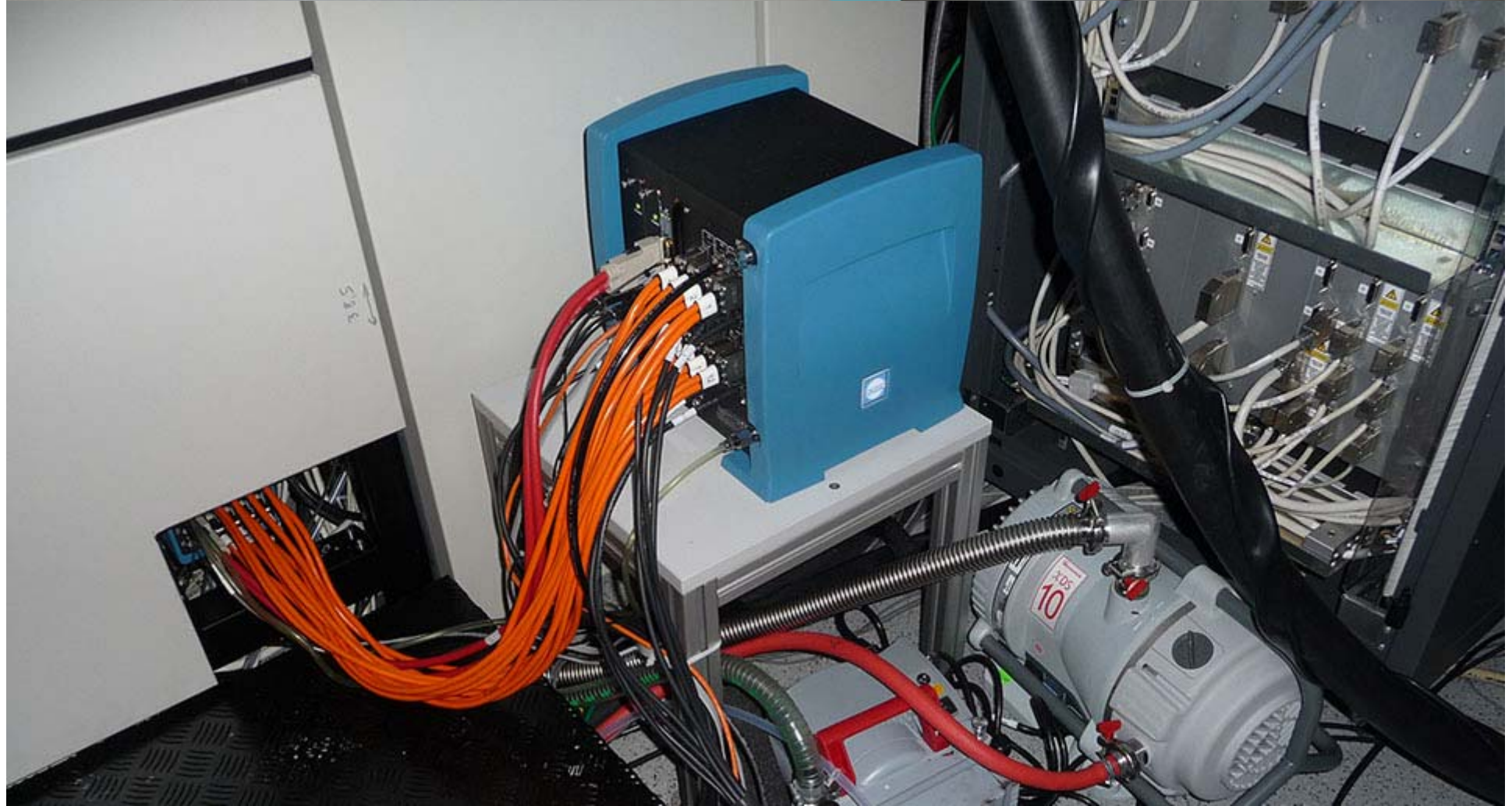
NAD filtered slice from tomogram
~ 30 % compression

Polara 300 KV, Mag: 55 KX, Pixel size: 0.55 nm/pixel, Def: -14 nm, Thickness: ~100 nm



Focused Ion Beam milling coupled to CET



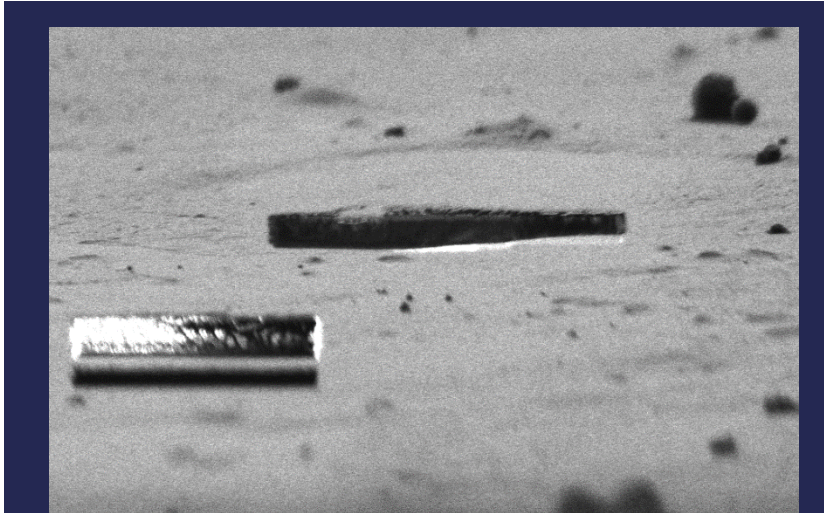


Advanced Transmission Electron Microscopy

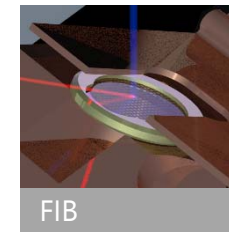
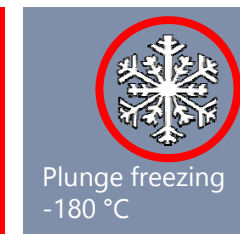
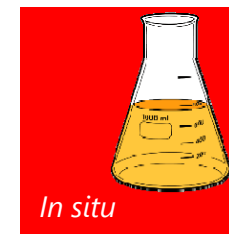
Dual-tilt axis CET with K2 camera and Energy filter



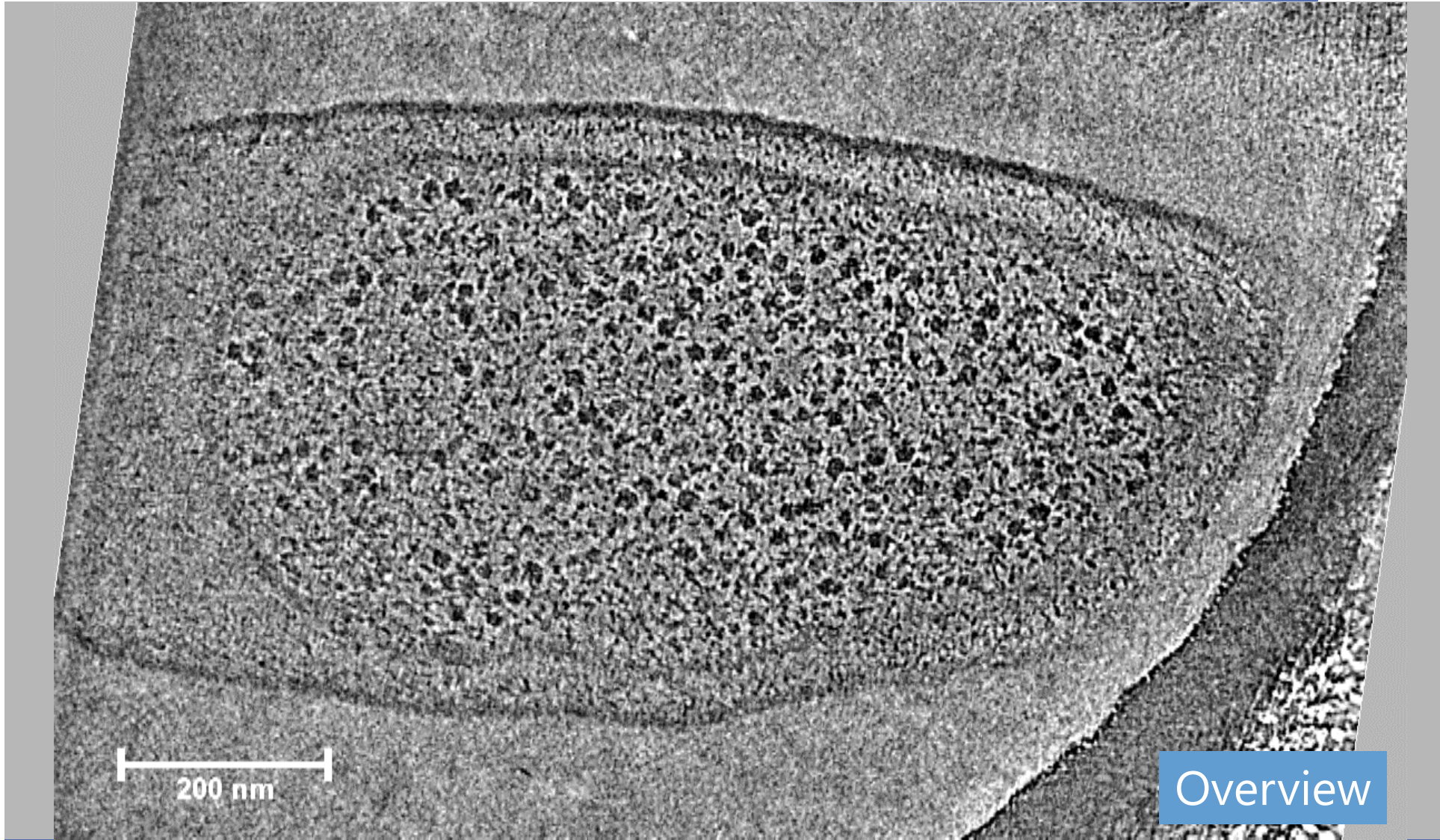
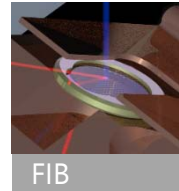
Polysomes *in situ*



Polysomes
E. coli



E. coli BL21 MtlA₃₈₅-SecM (non-stalling conditions)



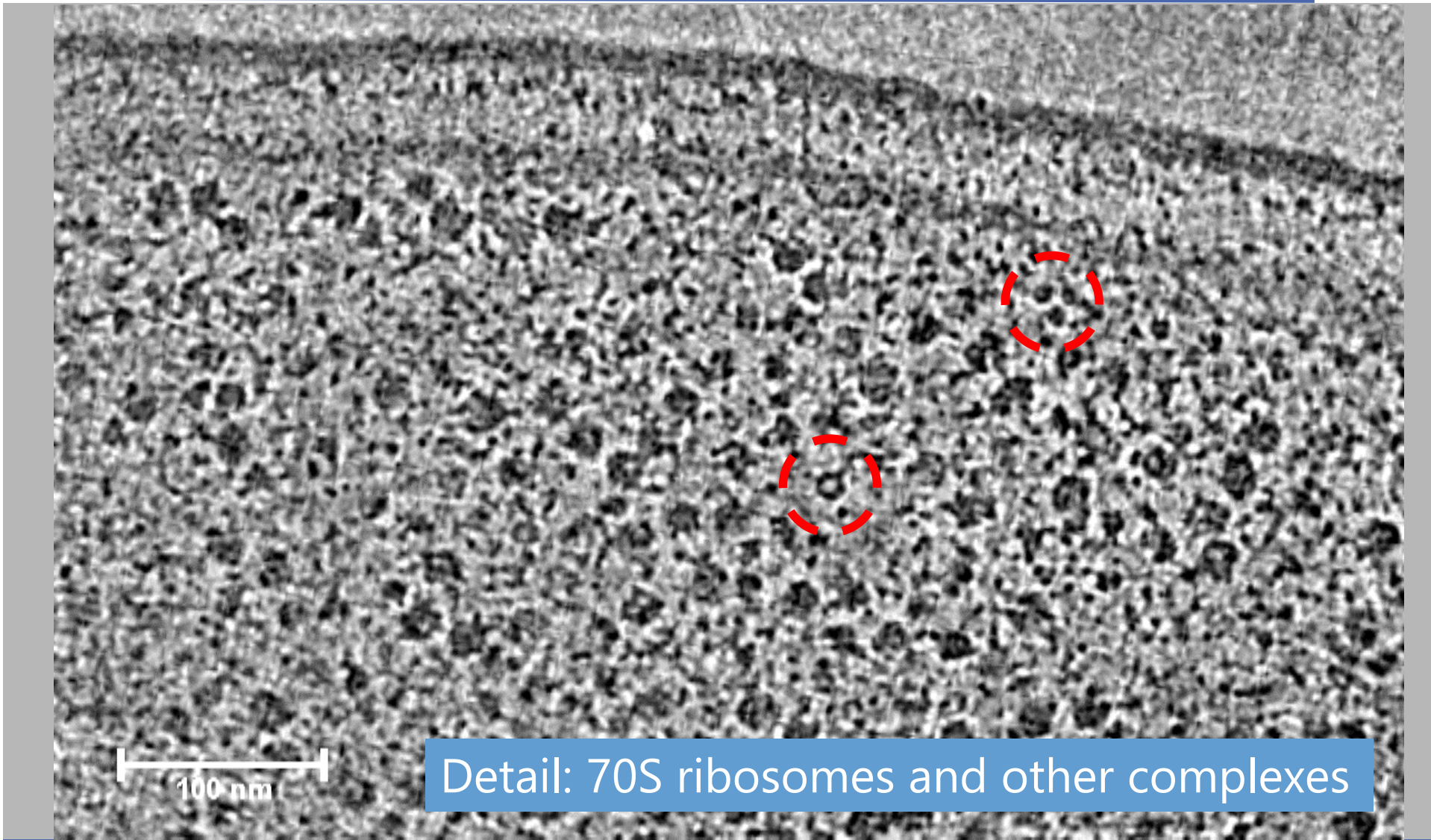
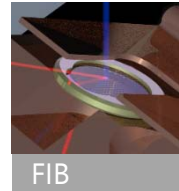
200 nm

Overview

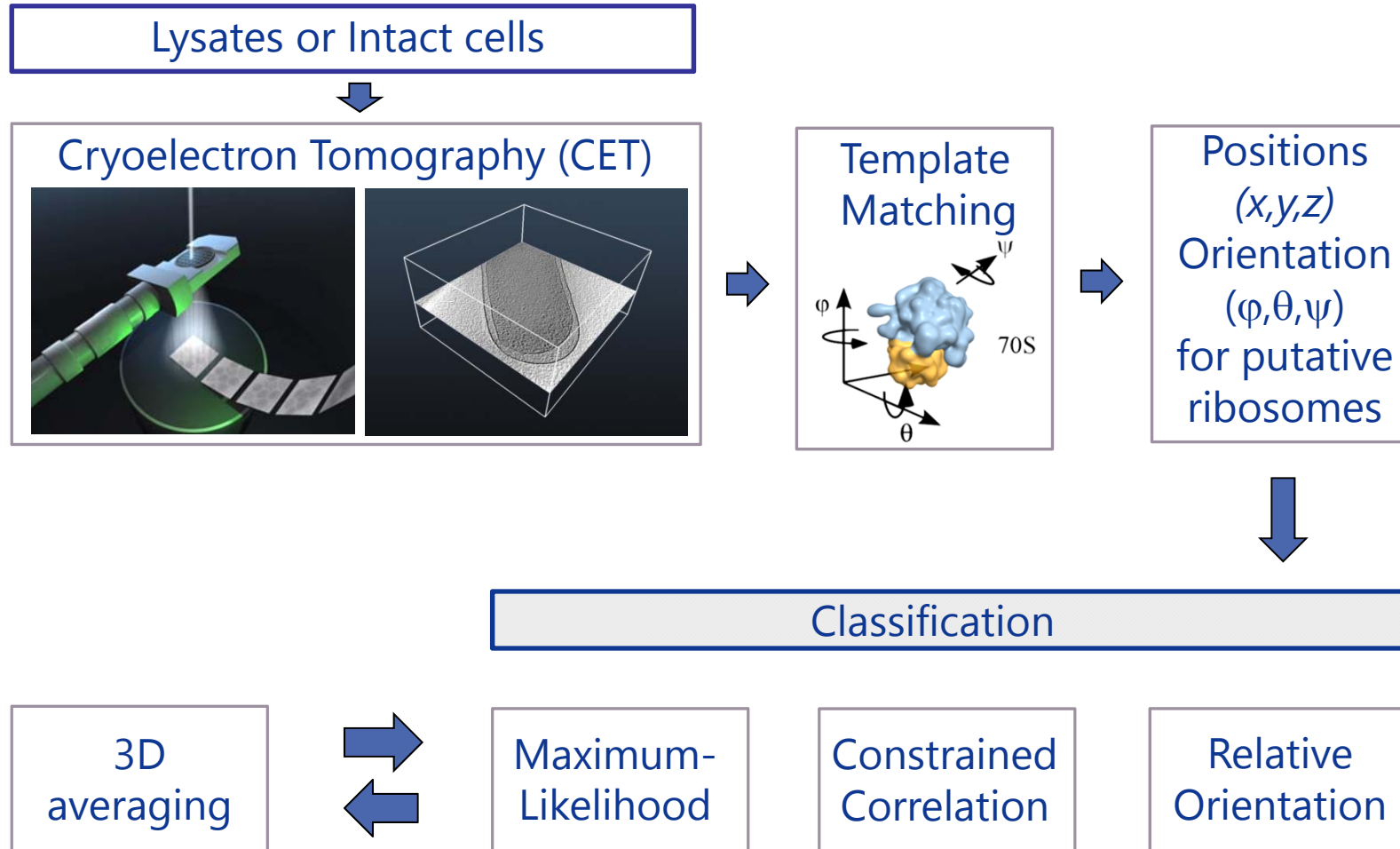


15

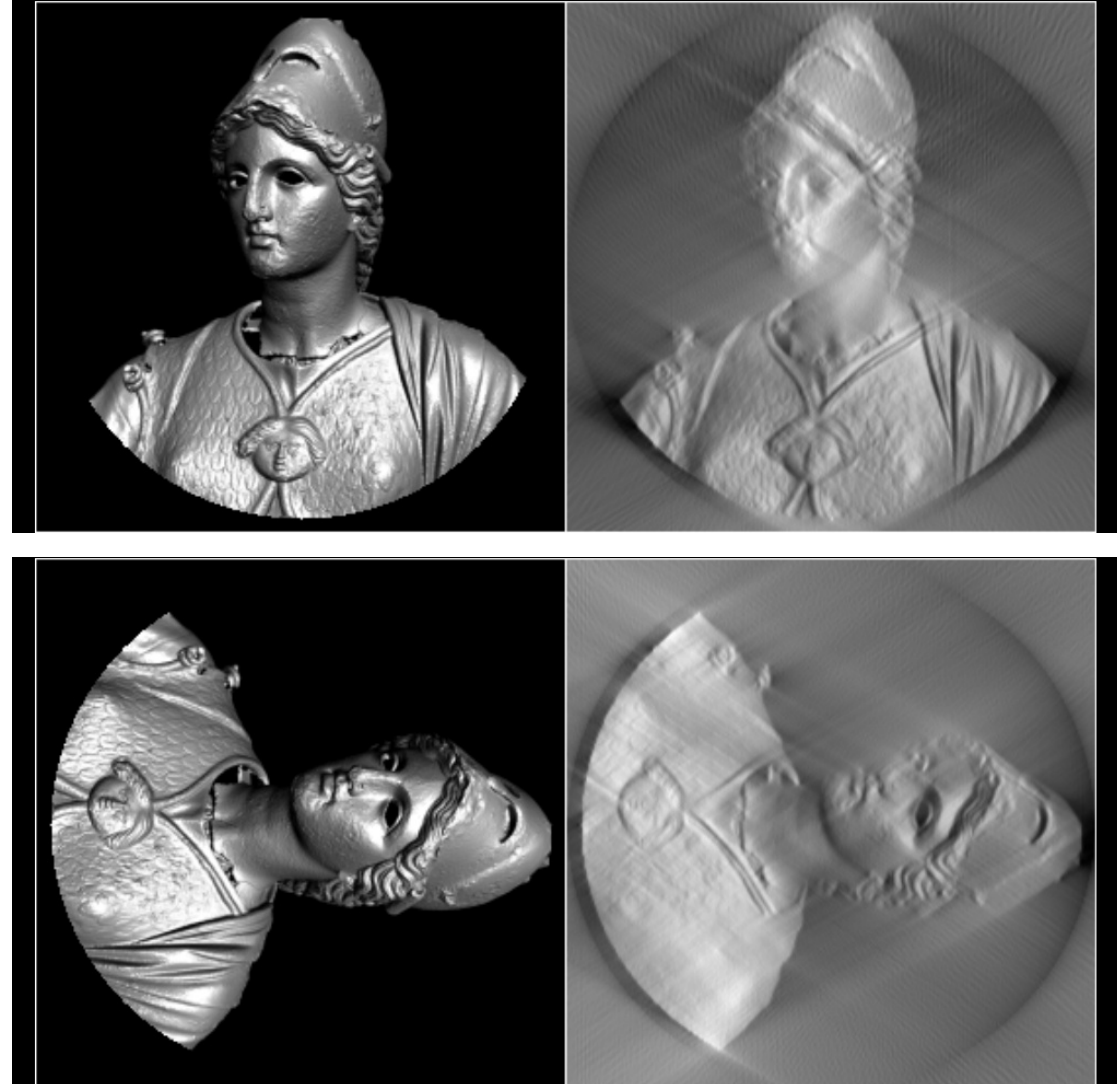
E. coli BL21 MtlA₃₈₅-SecM (non-stalling conditions)



Methods



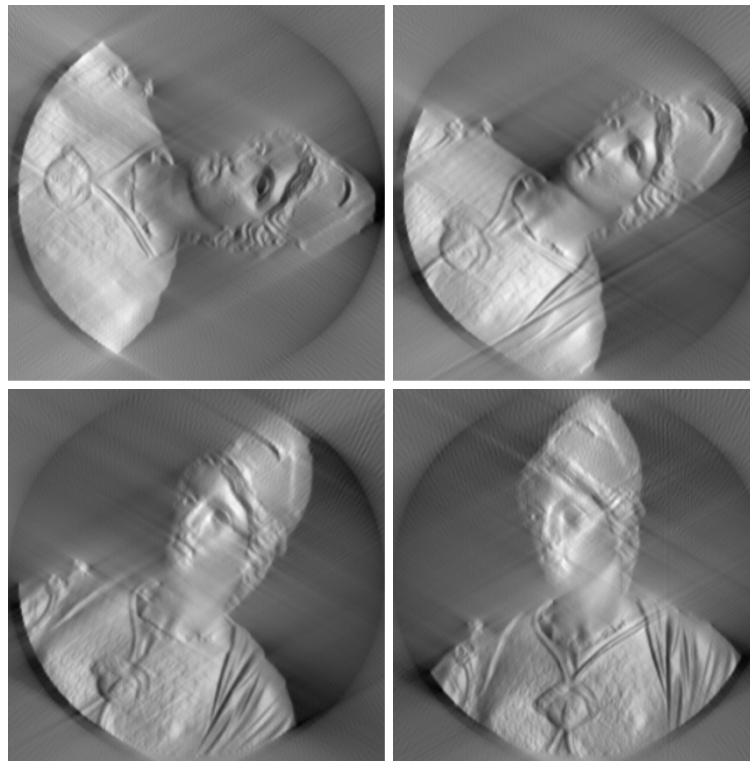
The art of averaging: Missing Wedge effect



Combining reconstruction by averaging



2D Model



Reconstructions from identical objects
in different orientations

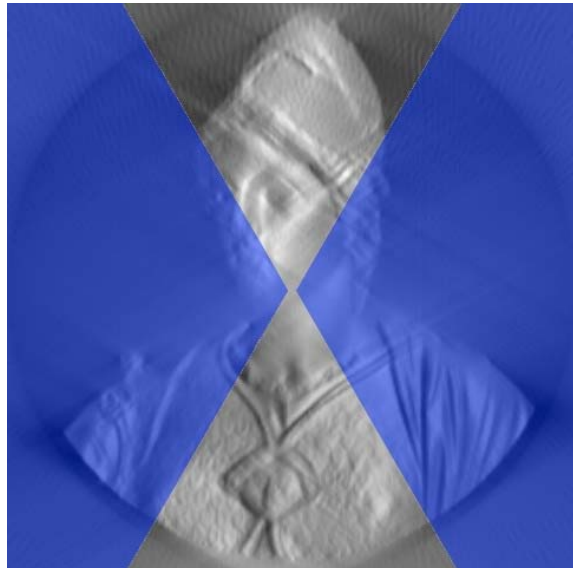


Combined reconstruction



The art of averaging

Combining objects in different orientations...

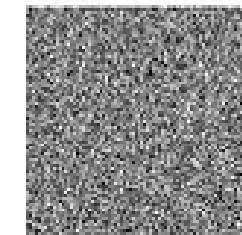


The art of averaging: The “Mona Lisa” effect – Bias caused by reference

template



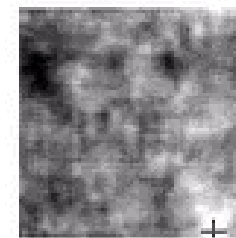
data



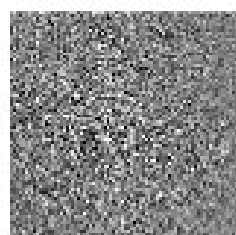
data aligned



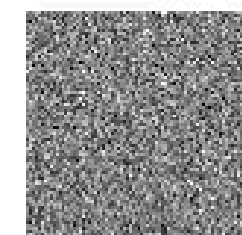
cross correlation



aligned average

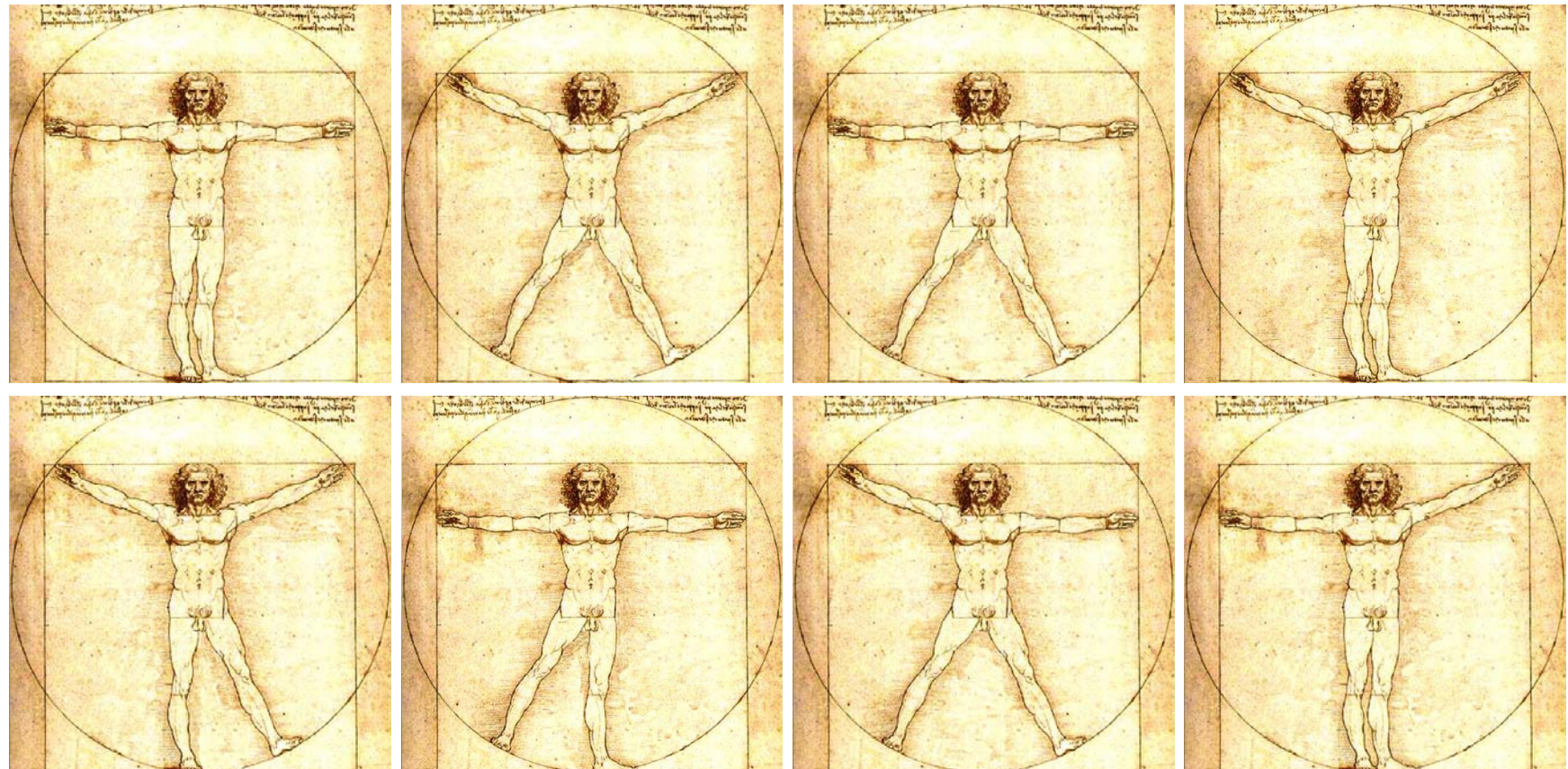


average



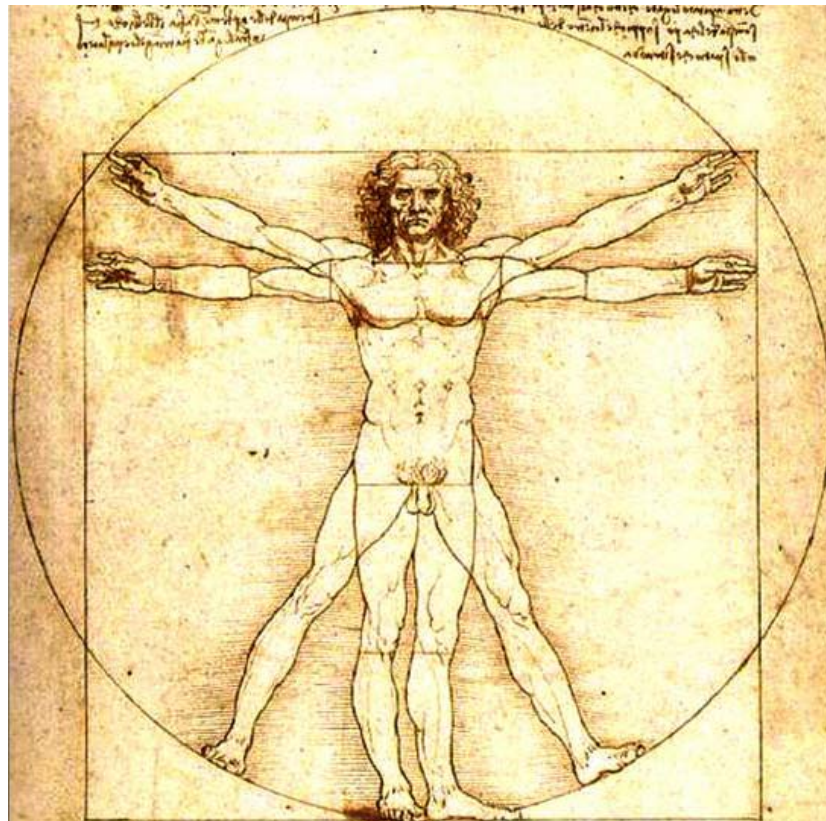
The art of averaging

The “Vitruvian man” effect – Flexibility and occupancy problems

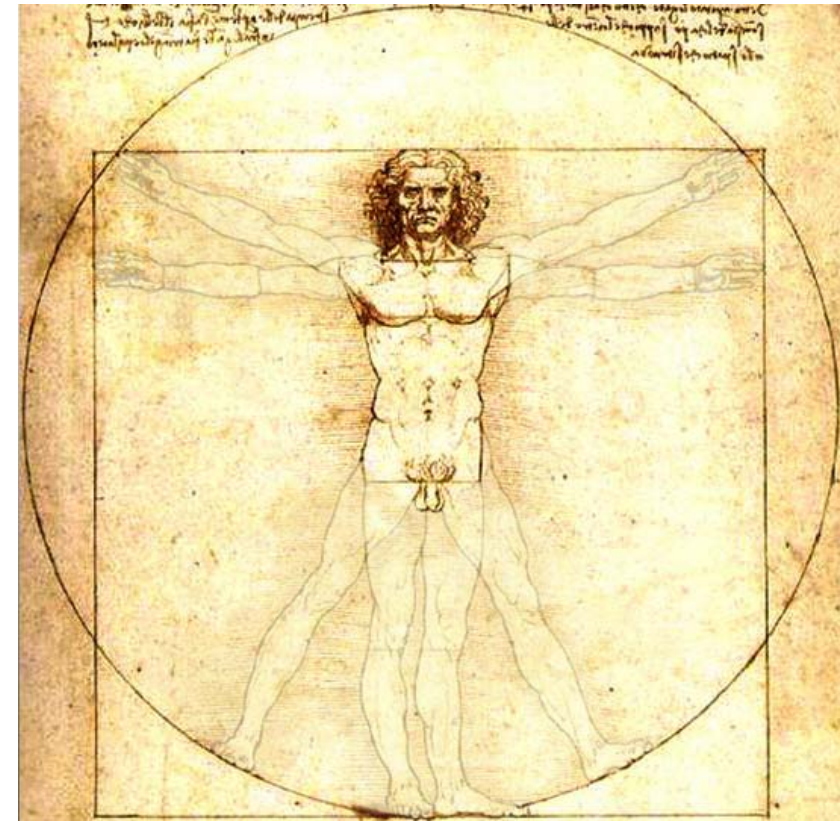


The art of averaging

The “Vitruvian man” effect – Flexibility and occupancy problems



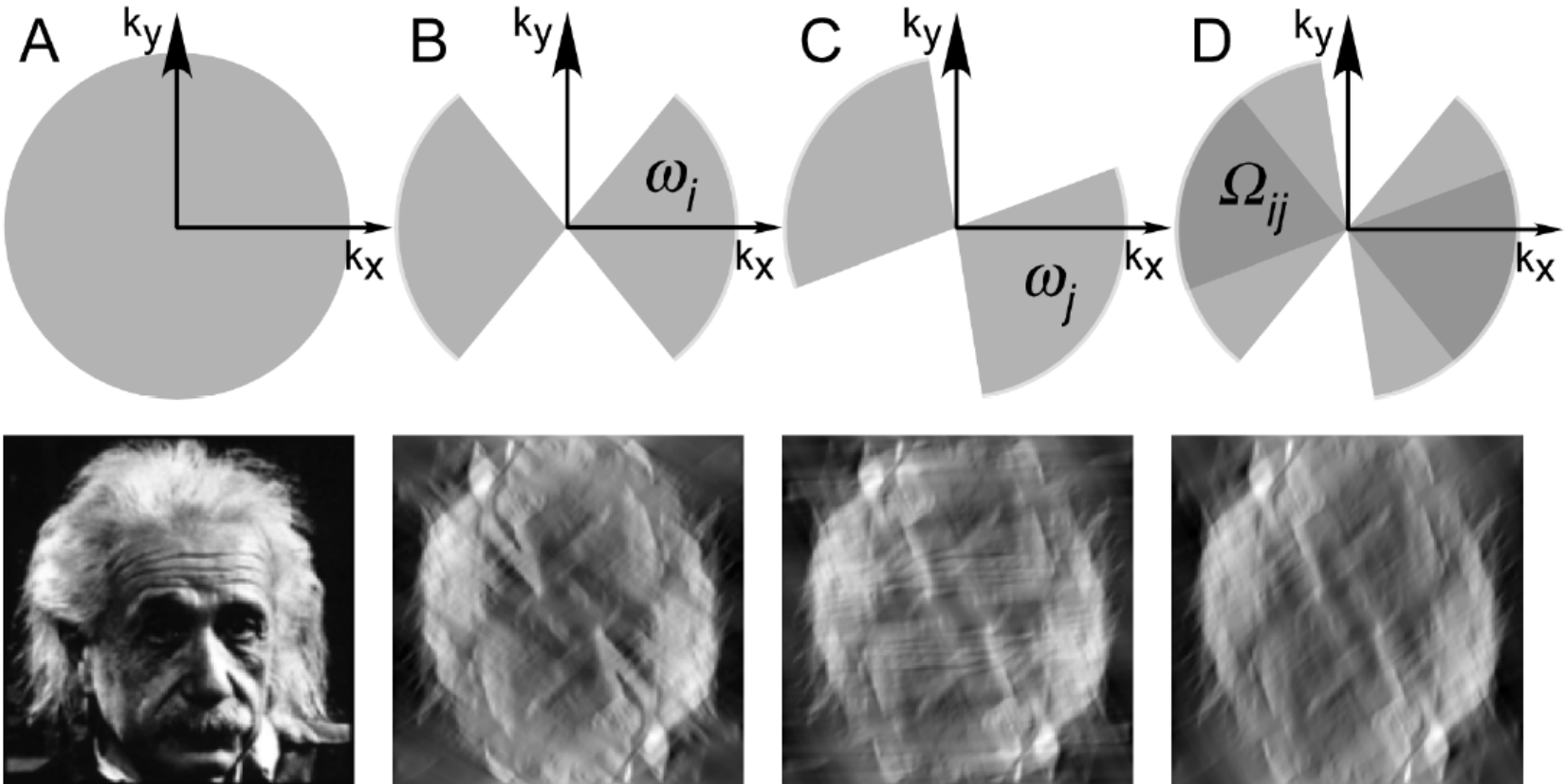
“Vitruvian man” – Leonardo Da Vinci



Average of 8 different images



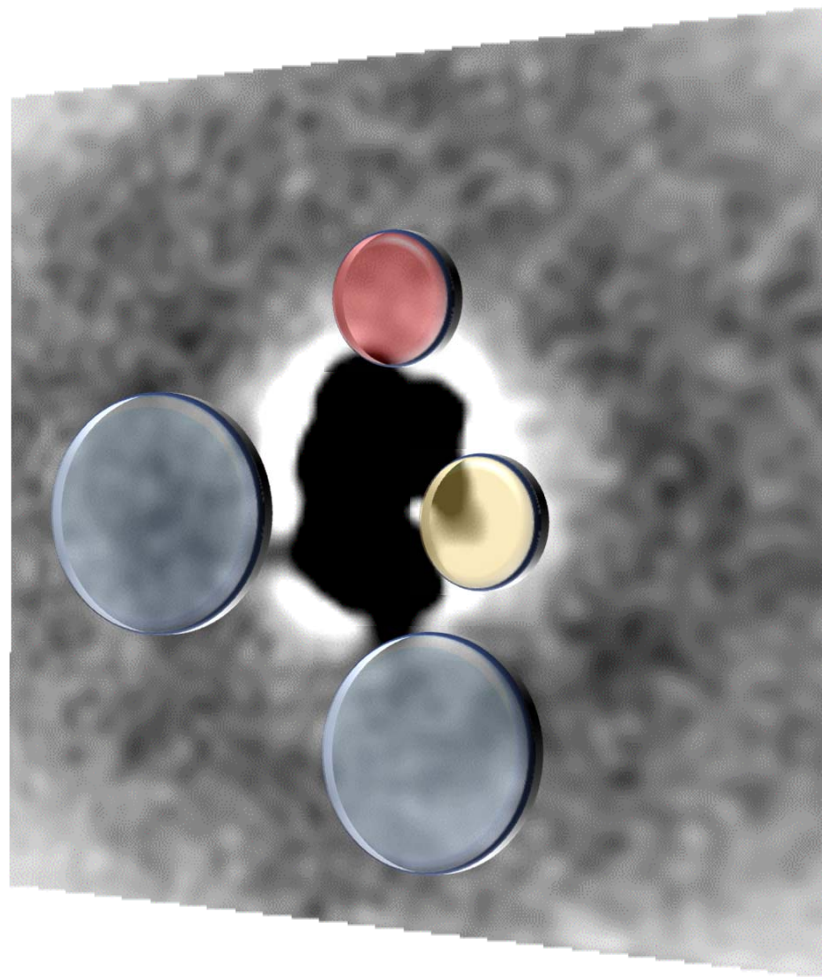
Constrained Correlation Classification



Förster F., et al. (2007) J. Struct. Biol.



Constrained Correlation Classification (3D-average selected ribosomes)



70S ribosome

Average of ~ 6000 part.
selected by
30S subunit similarity
resolution: ~2.6 nm

Areas with associated densities:



mRNA entry and
exit site



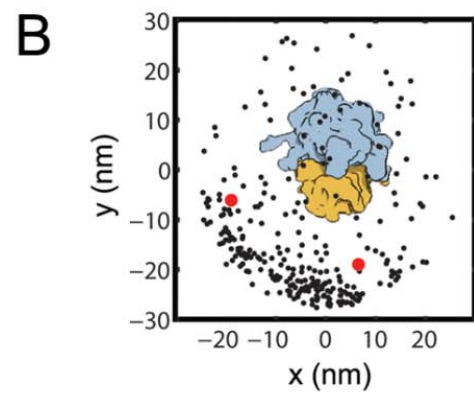
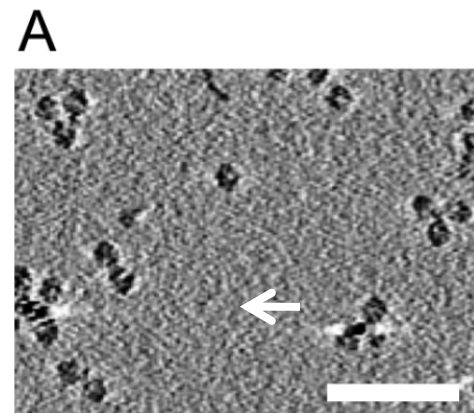
Elongation factor
binding sites



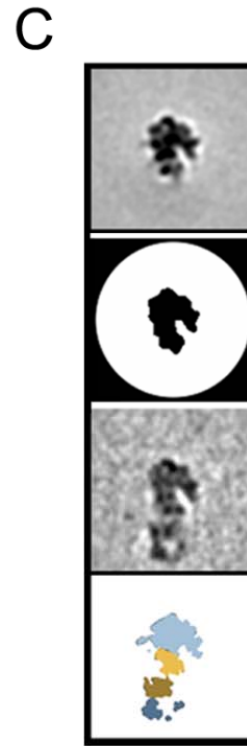
Nascent chain
exit site



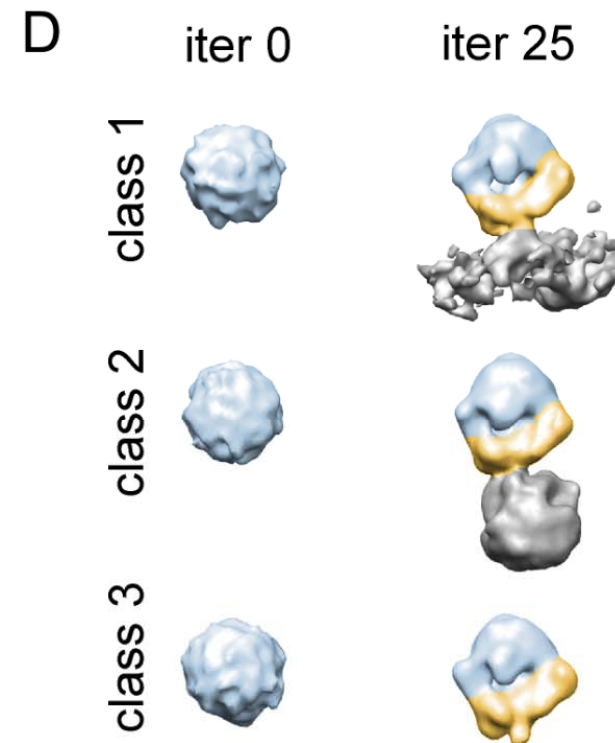
Hibernating Ribosomes in Lysates from Starved *E. coli* Cells



Relative
Orientation



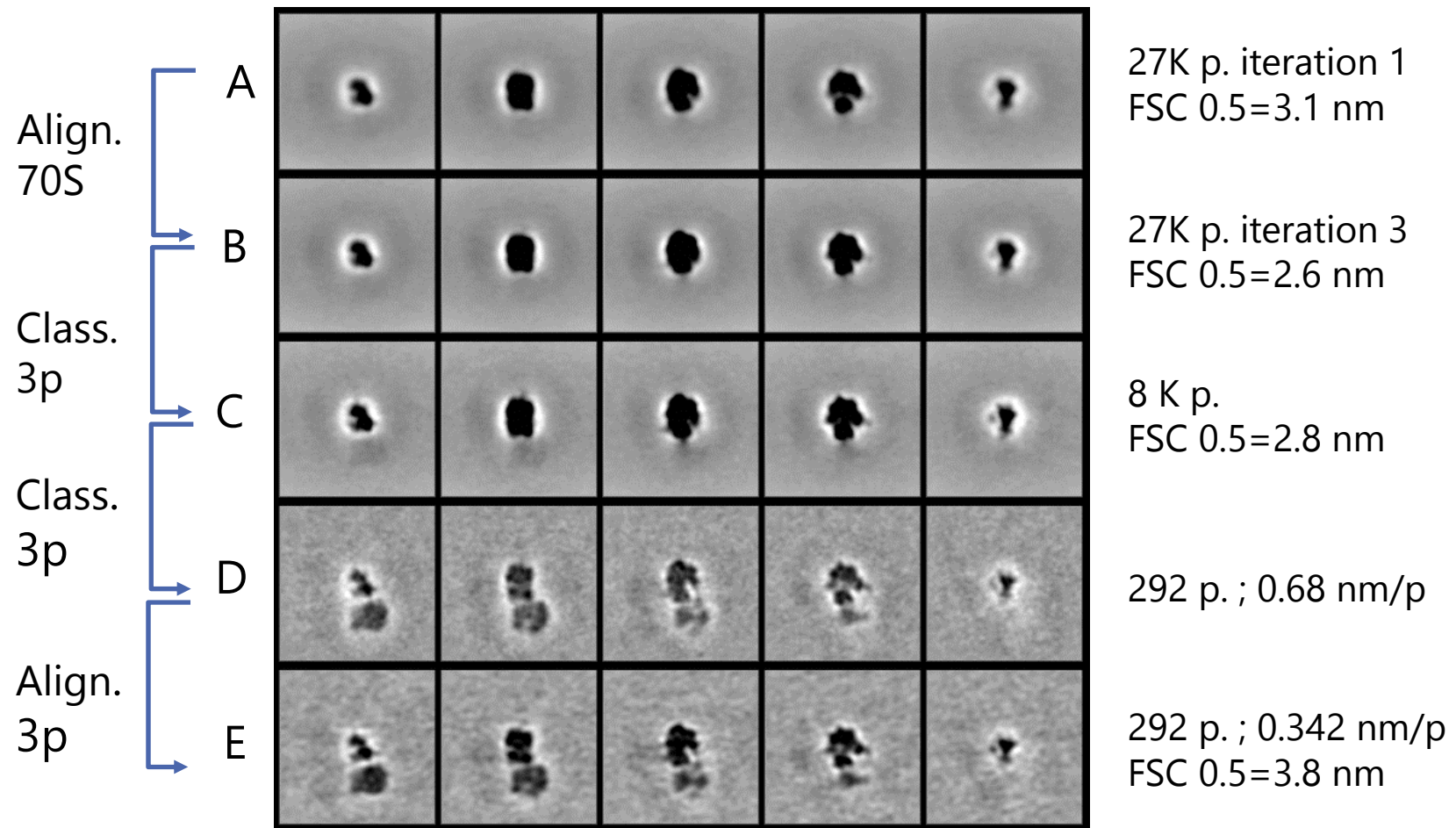
Constrained
Correlation



Maximum-
Likelihood



3D Alignment and Averaging



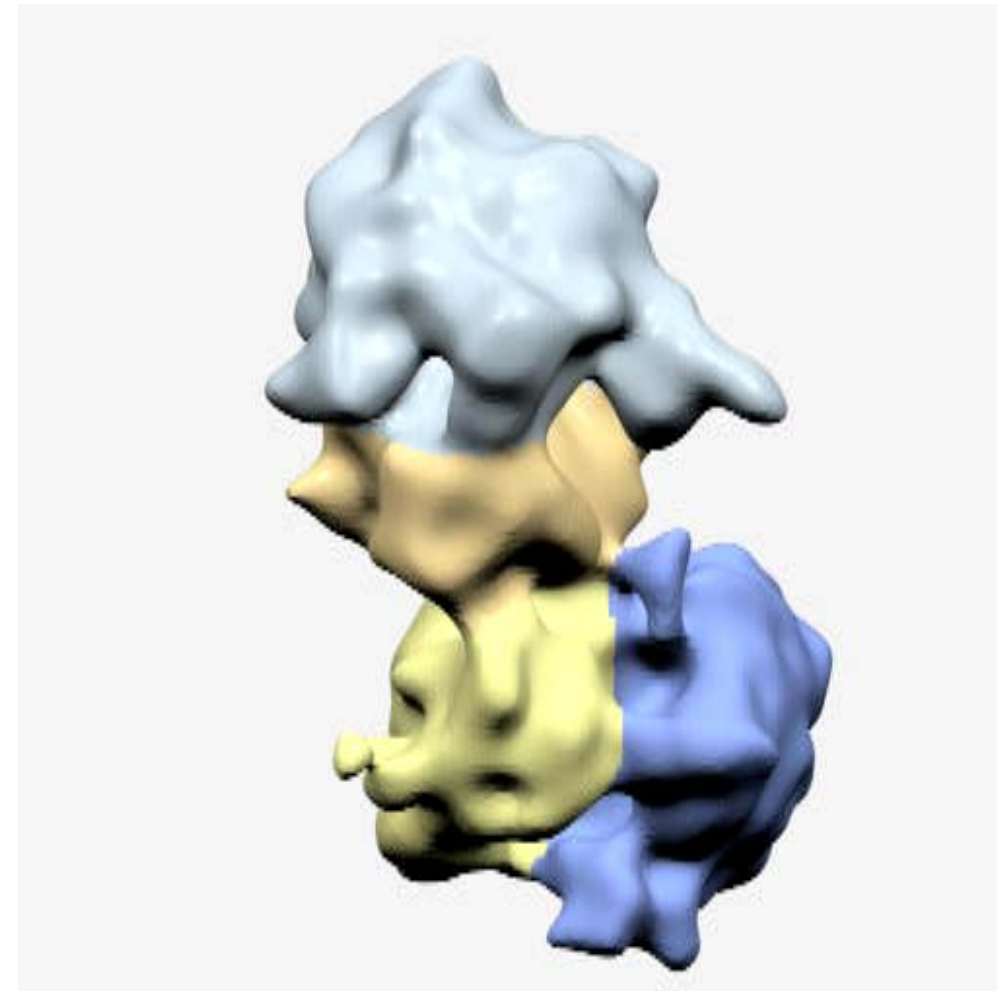
3'-neighbor ribosome attached in ca. 1% of analyzed particles



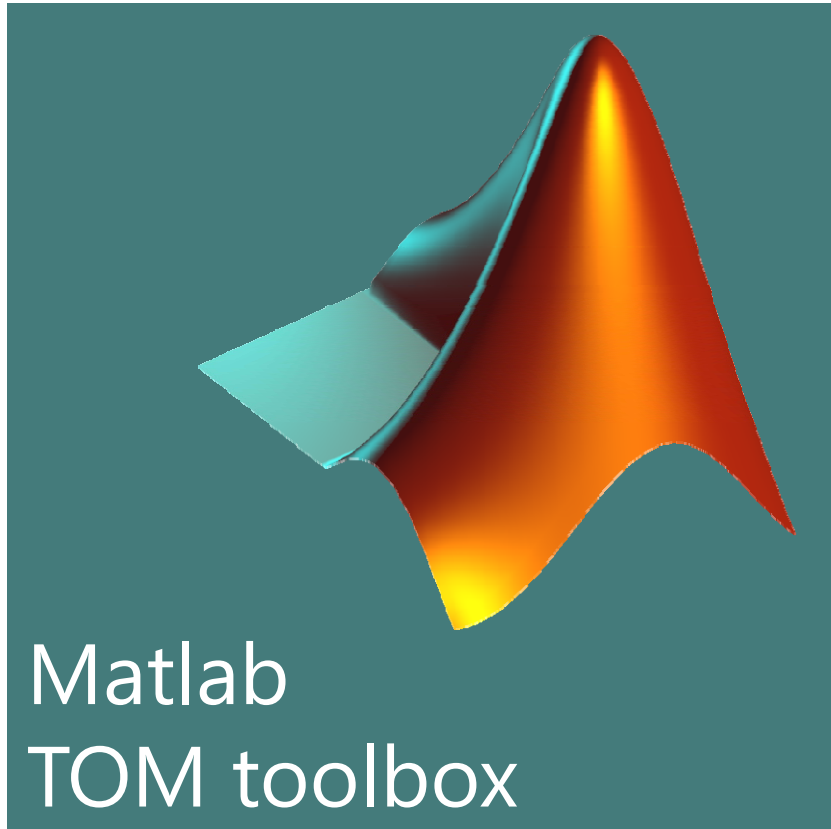
Polysomal organization *in situ*: 3D-Average “top-to-top”

- 103 particles
- $(256)^3 p$, 0,342 nm/p
- Average filtered at 3nm res.
- Particles present in all analyzed tomograms

- 50S - central ribosome
- 30S - central ribosome
- 50S – neighbor ribosome
- 30S – neighbor ribosome



Methods: Software



Matlab TOM toolbox

The toolbox supports a wide range of functions for tomography that extend the capability of the MATLAB® numeric computing environment.

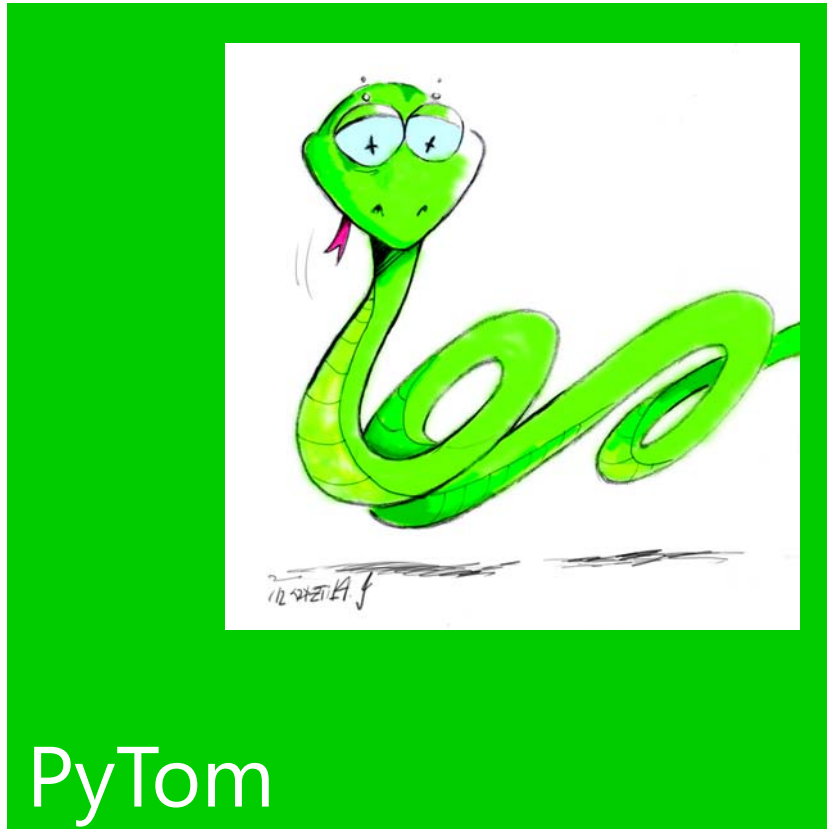
Aim:

Customable procedures for tomogram reconstruction and analysis.

Nickell. S. et al. (2005) *J. Struct. Biol.* **149**:227-34



Methods: Software



PyTom

Open-source platform that unifies standard tomogram processing steps in a single python-based toolbox.

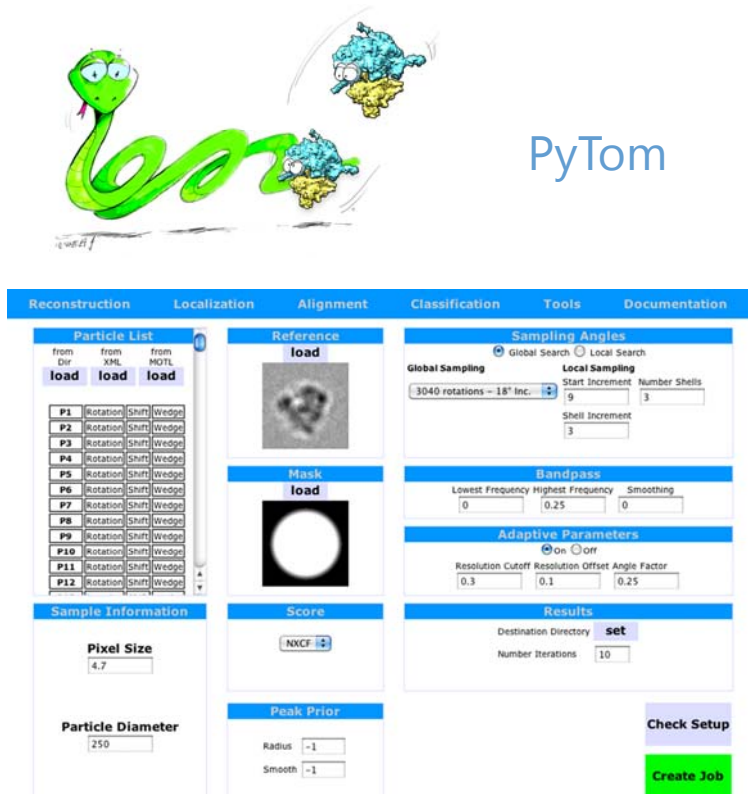
Aim:

3D alignment, averaging and classification of subtomograms.
Implementation of new algorithms for image processing in ECT.

Hrabe, T., et al. (2012) JSB 178: 177-188



Recent Improvements in Data Processing Workflow



Hrabe, T., et al. *J. Struct. Biol.* 2012

1. Reconstruction

- Phase Flipping ('CTF correction')
- Projection Alignment
with Tilt-Specific Image Rotation + Magnification

2. Localization

- Template Matching (+Support Vector Machines)
- Parallel processing on LINUX cluster
- Better angular sampling

3. Subtomogram Alignment

- Parallel processing on LINUX cluster
- Resolution-dependent lowpass: low bias
- Resolution-dependent sampling
- Direct reconstruction from projections

4. Classification

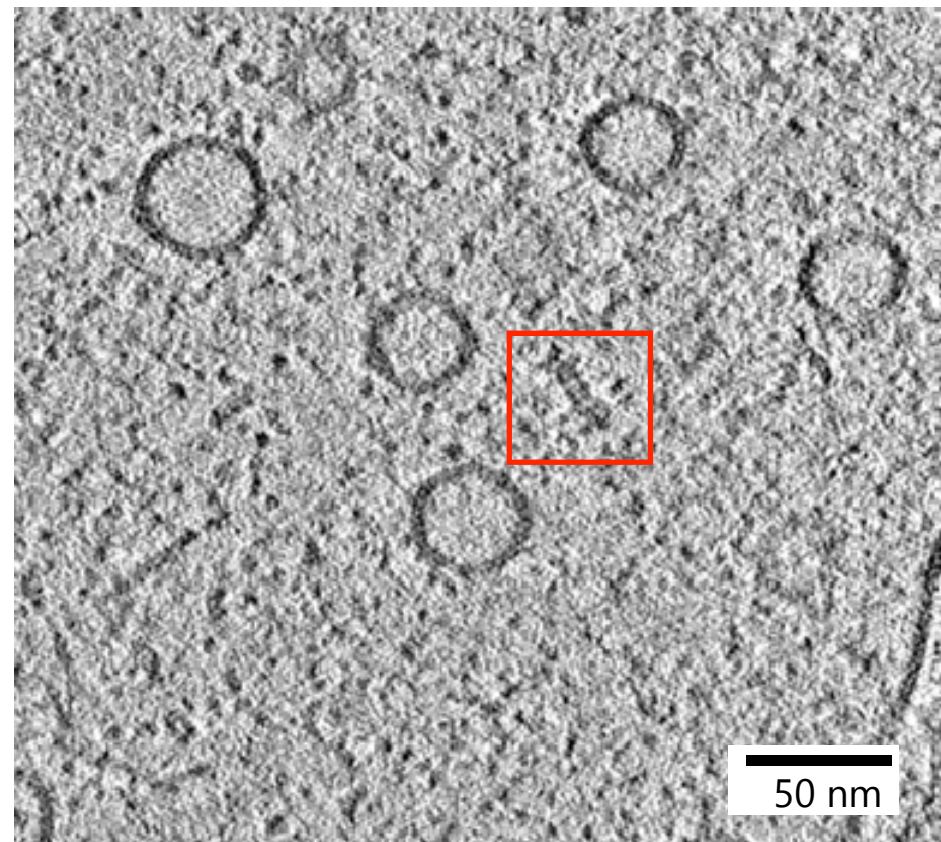
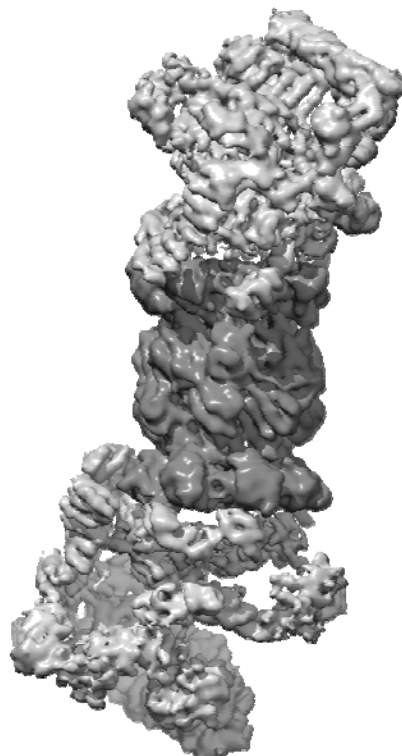
- Multi-reference correlation with simulated annealing



CET: Direct detection and Phase Plates

Asano, S. et al. (2014) *Science* 347:347

Sample: Hippocampal primary cultured neuronal cell



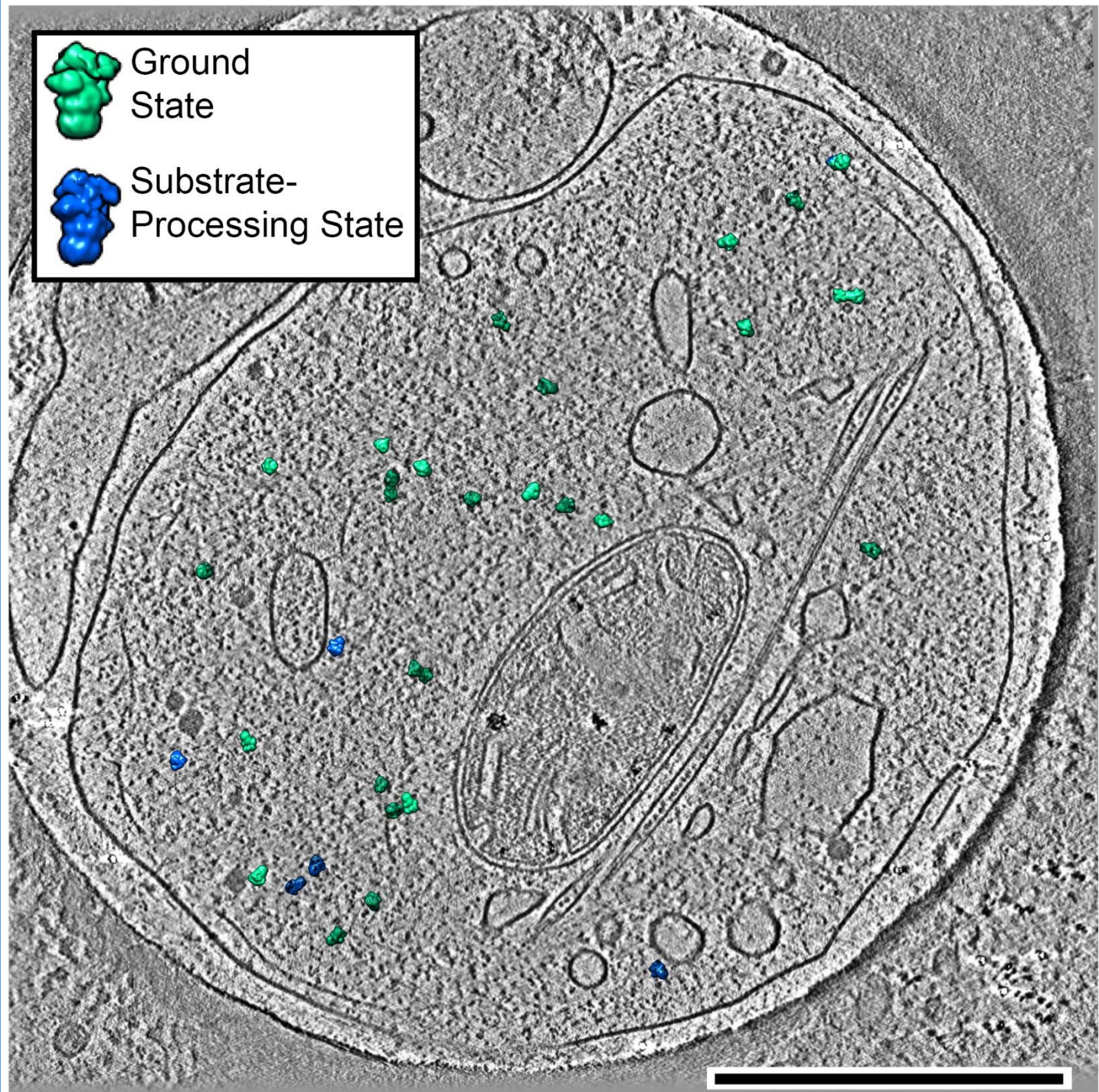
26S Proteasome *in situ*!





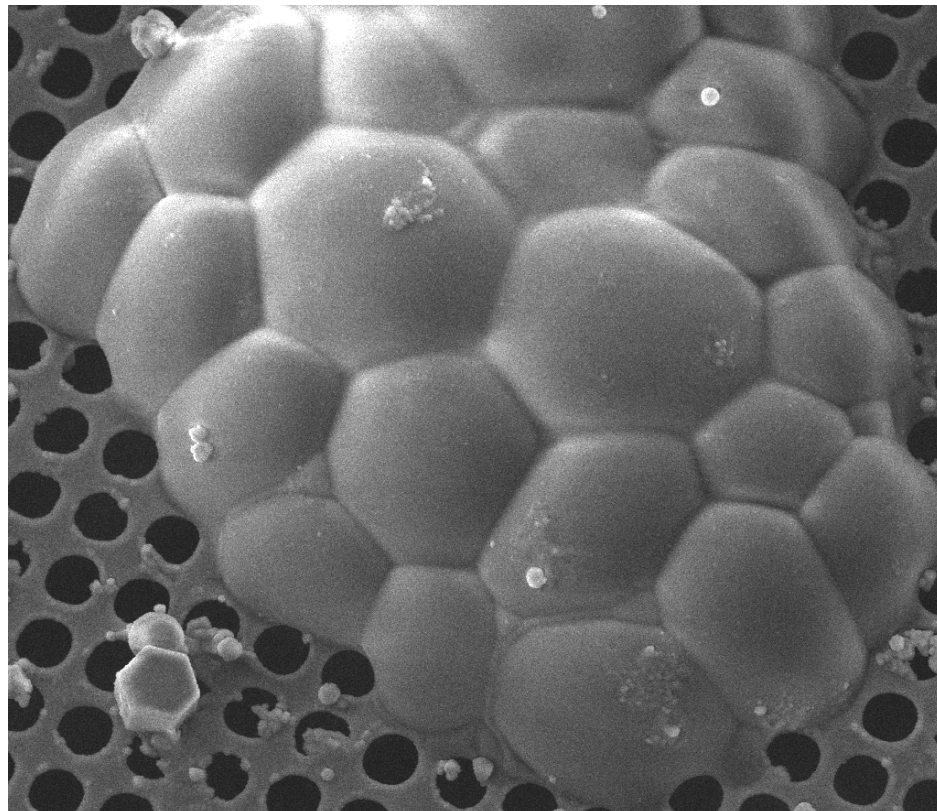
Proteasomes in neurons cytoplasm

Asano, S. et al. (2015)
Science 23:347

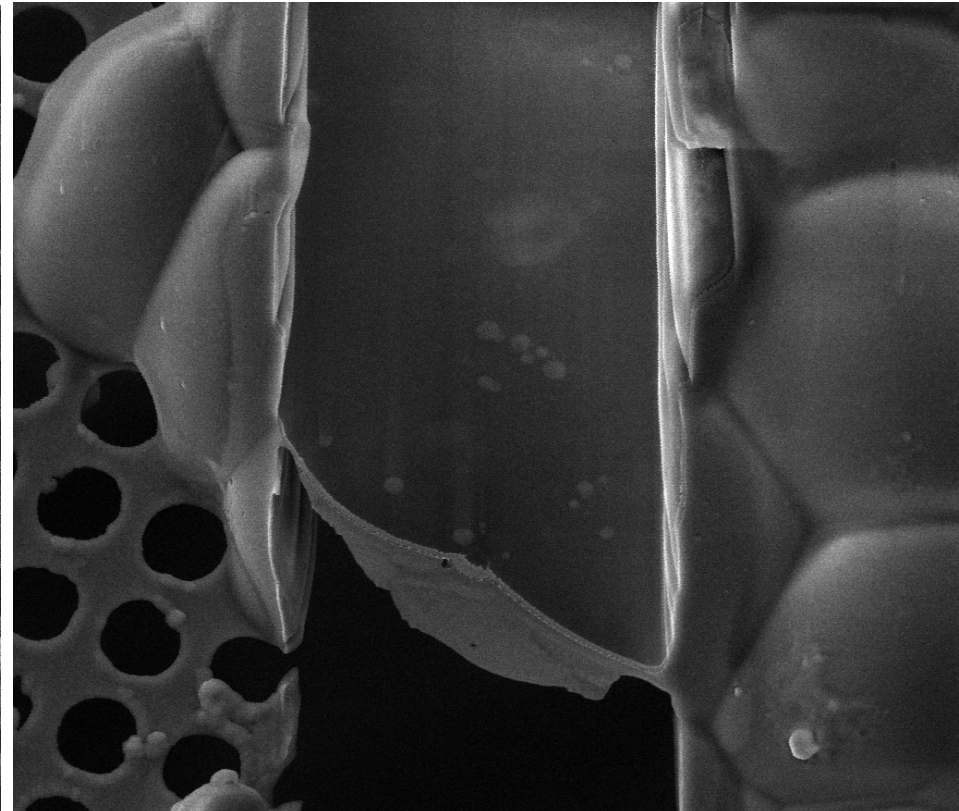


Cryo-FIB: *Chlamydomonas reinhardtii*

40 µm



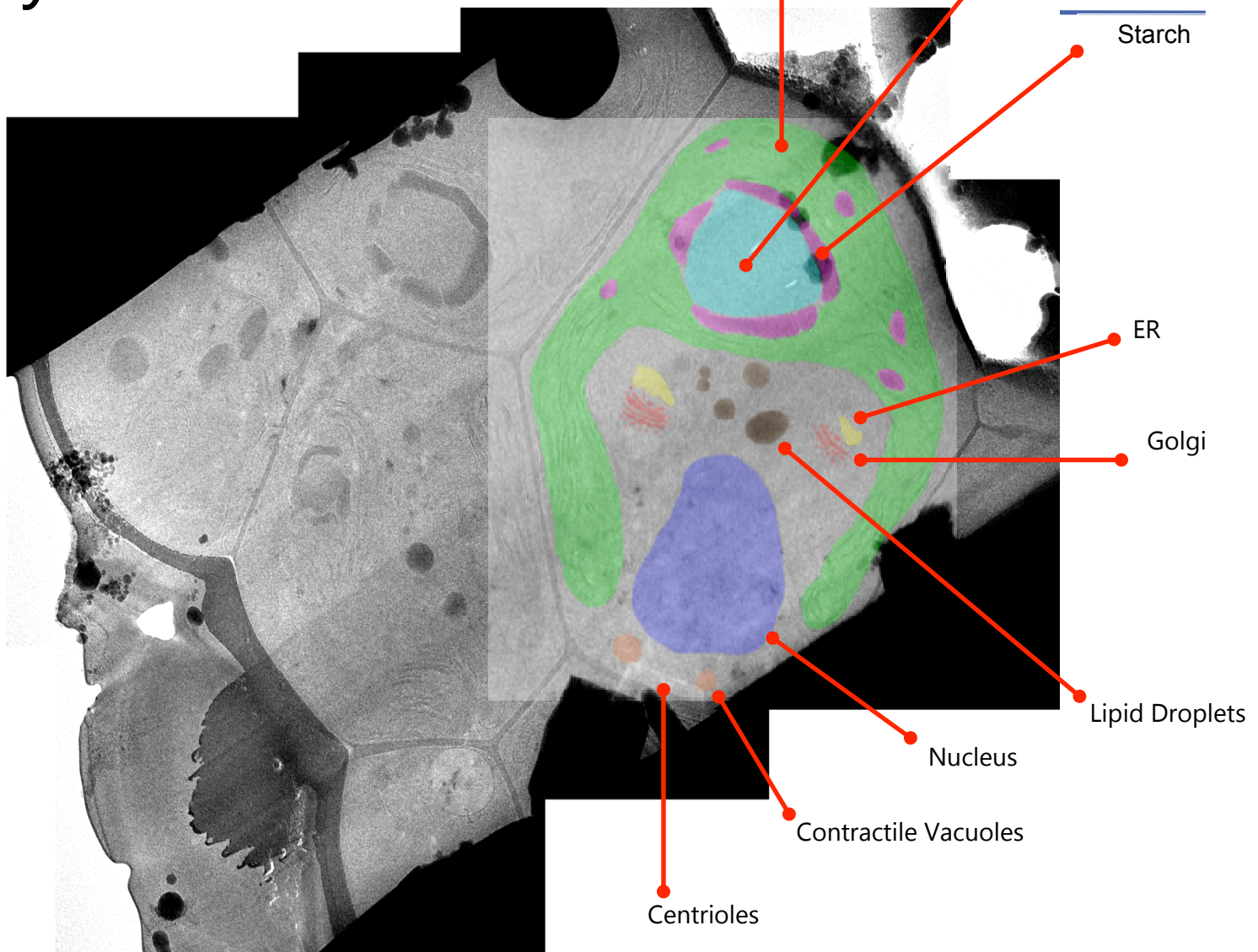
10 µm



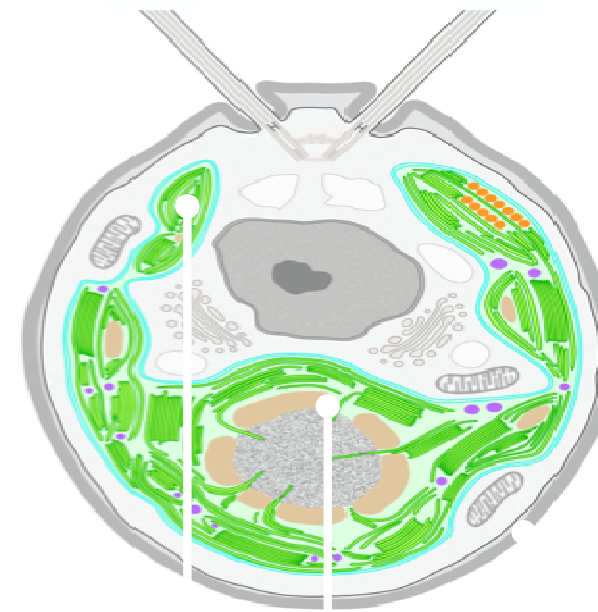
Engel, BD. et al. (2015) *Elife* 13;4



Cryo-FIB: Chlamydomonas



Cellular CET: 'fibbed' Chlamydomonas



Starch

Globules

Pyrenoid

Thylakoids

Engel, BD. et al. (2015) *Elife* 13;4



Cryo-FIB: *Chlamydomonas reinhardtii*

Engel, BD. et al. (2015) *Elife* 13;4

RuBisCO



CCD

Pyrenoid

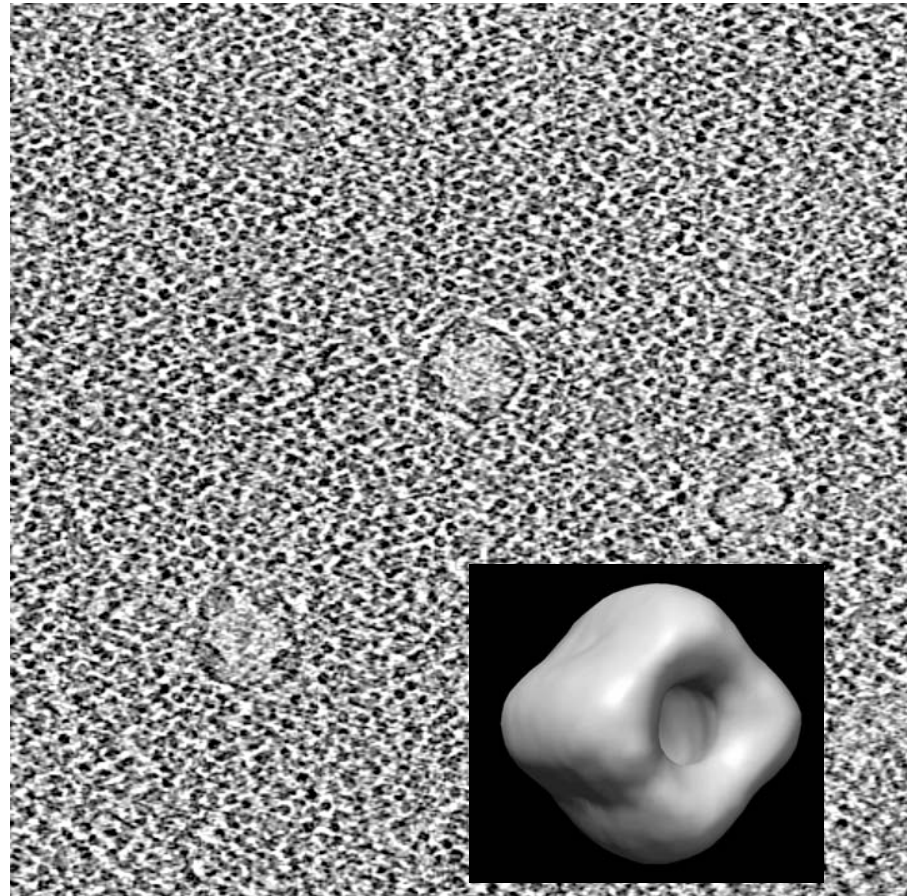


CRYO-FIB: *Chlamydomonas reinhardtii*

RuBisCO



CCD



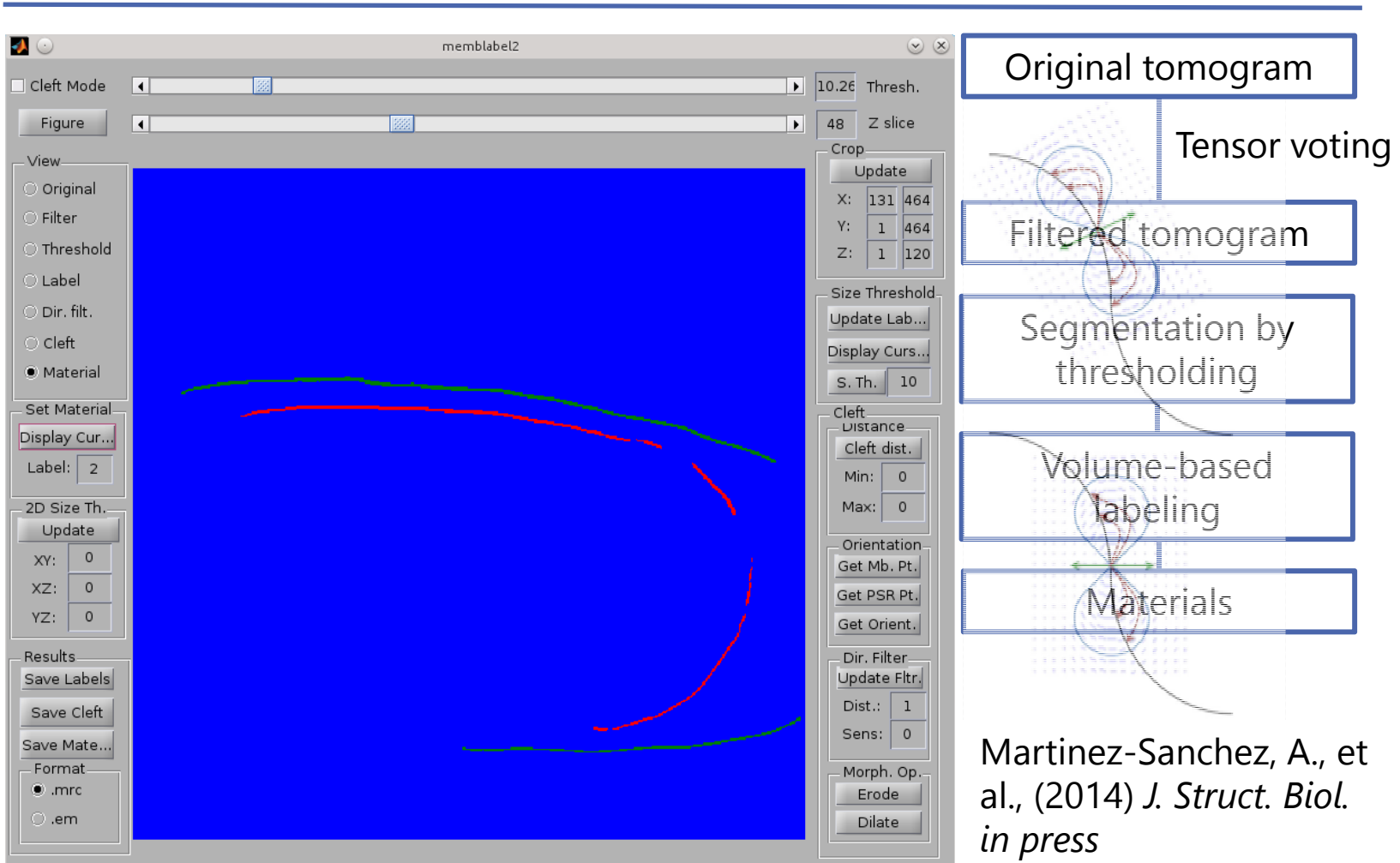
Pyrenoid

K2 Summit

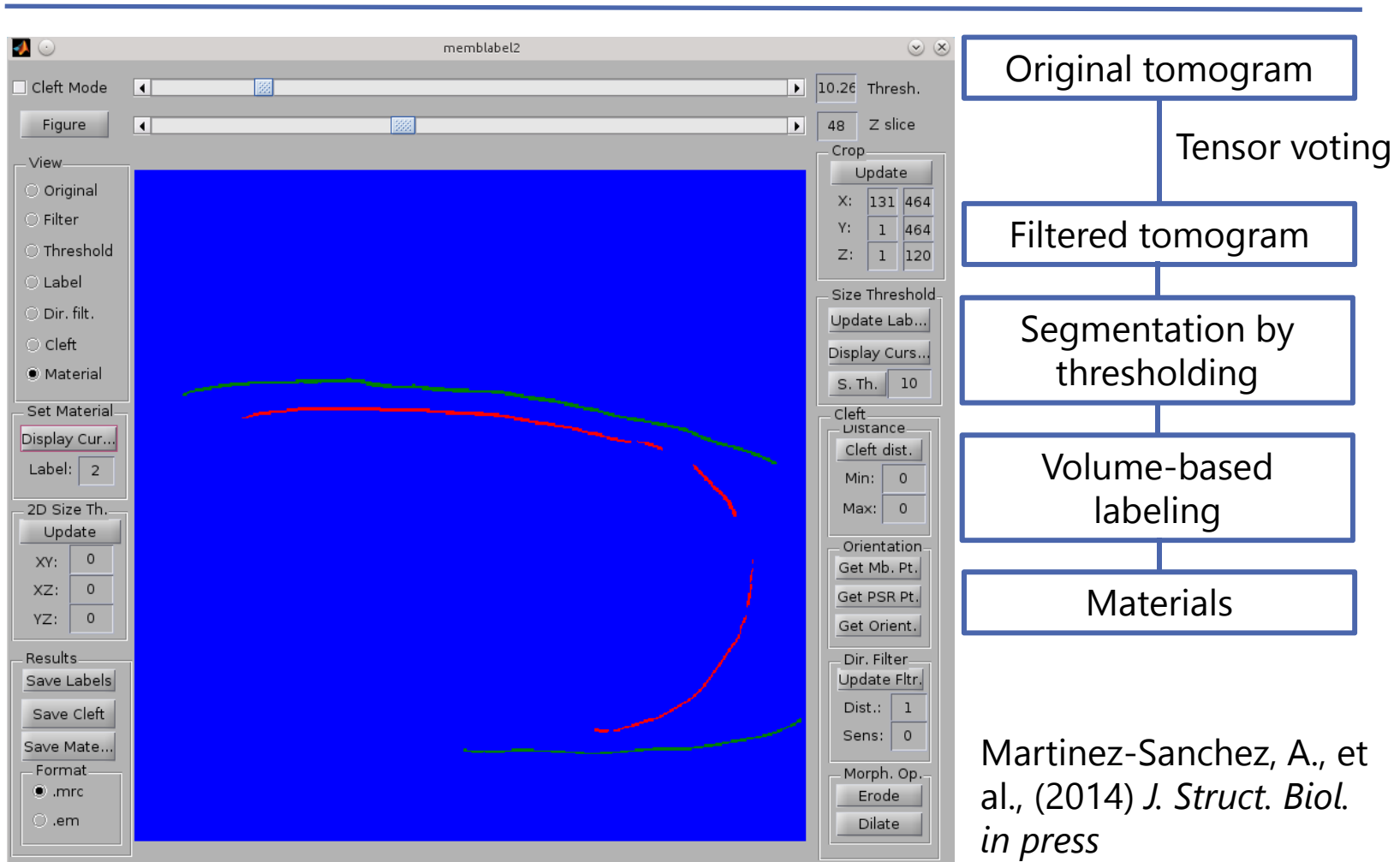
pixel size: 0.424 nm; 10,000 particles out of ~300,000 from ONE
tomogram



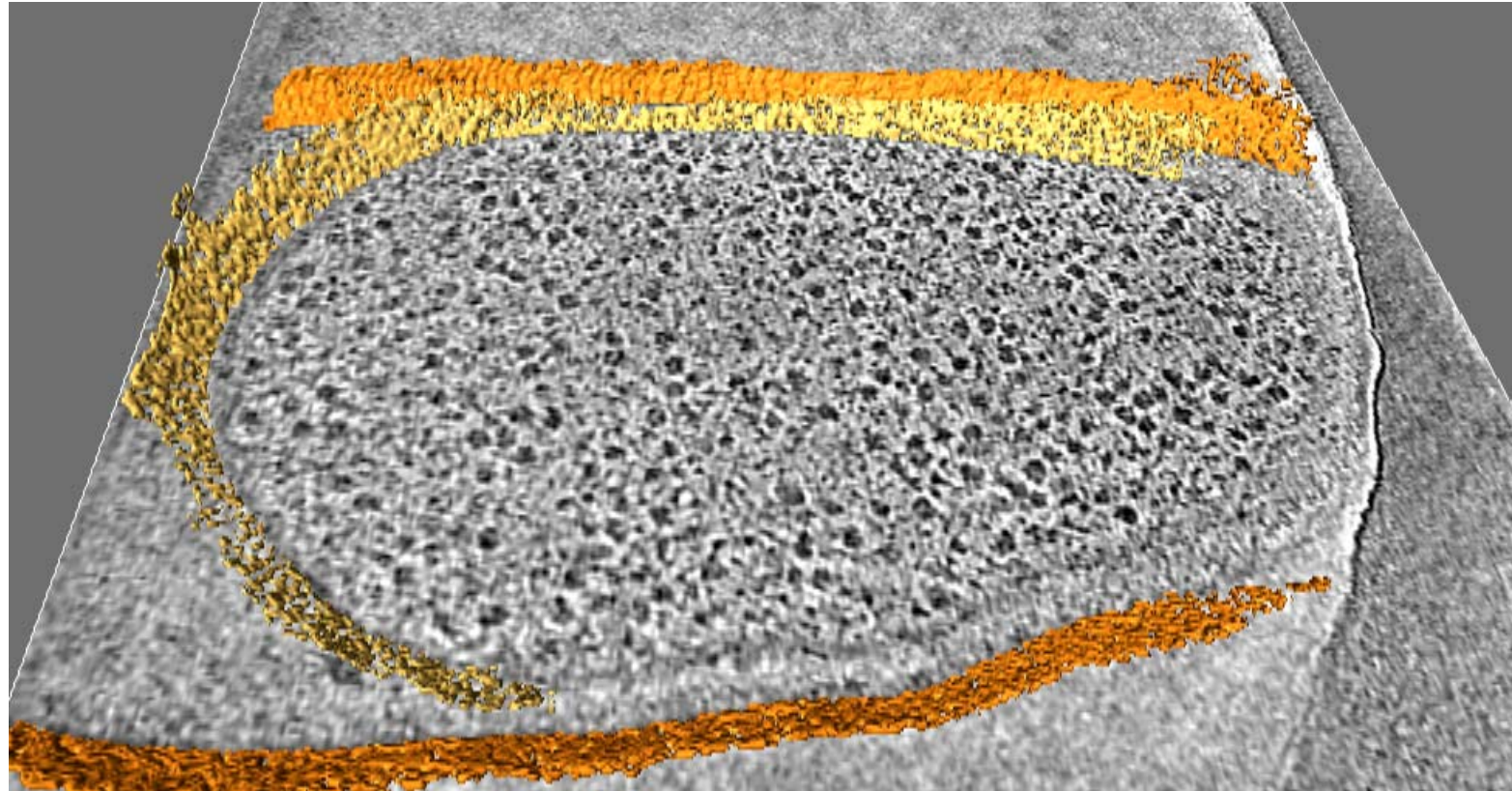
Robust membrane segmentation based on tensor voting



Robust membrane segmentation based on tensor voting



Robust membrane segmentation based on tensor voting

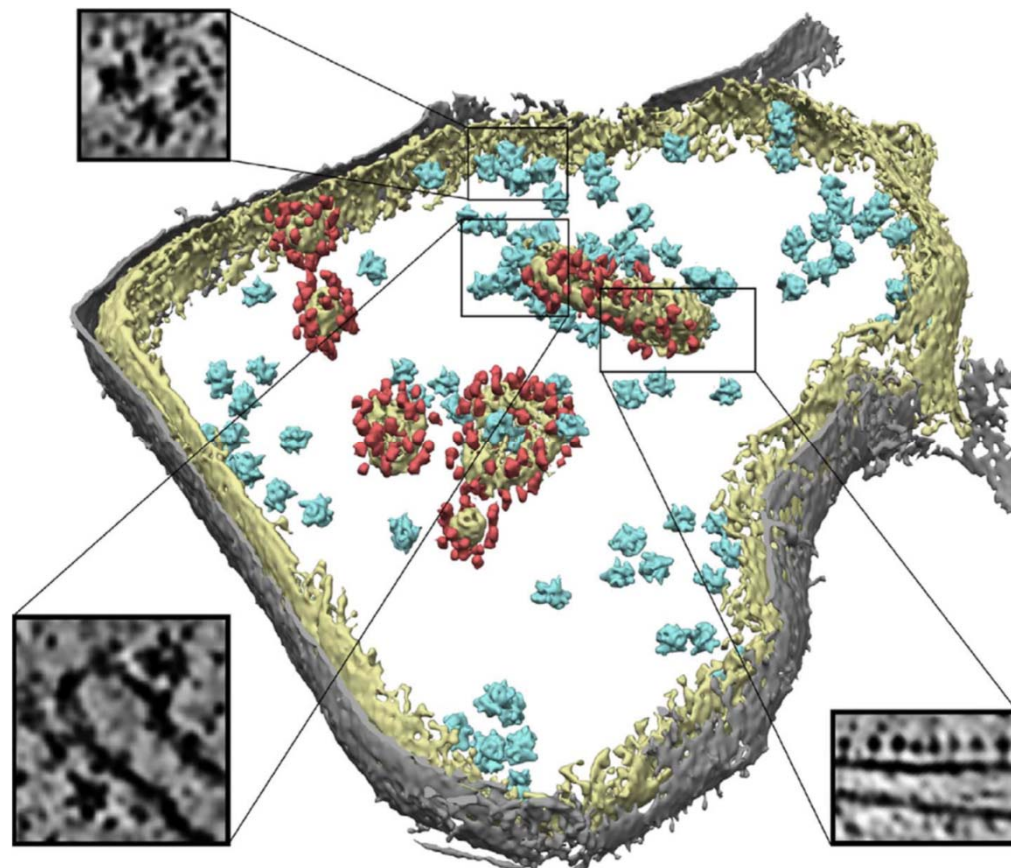


segmented outer membrane

segmented inner membrane



Organization of the mitochondrial translation machinery studied *in situ* by cryo-electron tomography

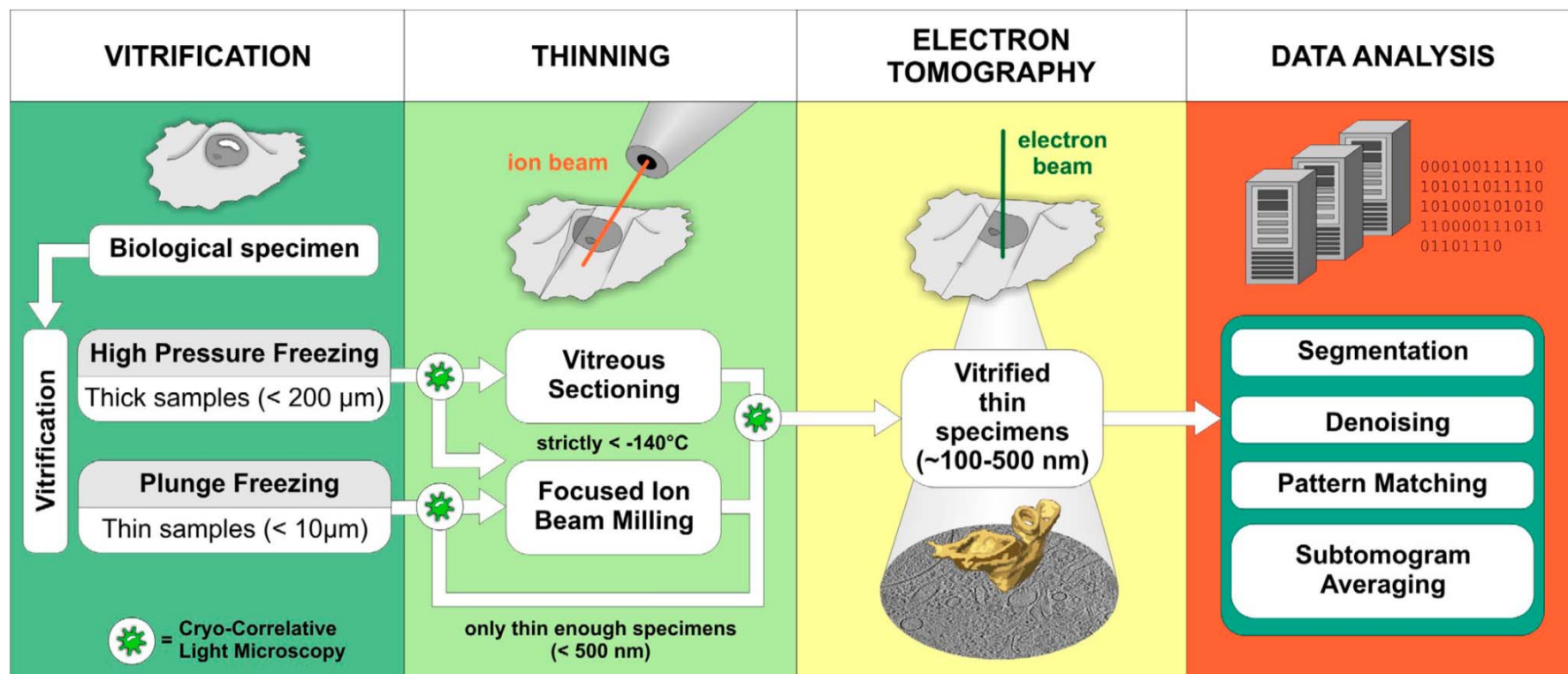


Distribution of mitoribosomes in translation-competent yeast mitochondria.

Pfeffer, S. et al., (2015)
Nature Communications



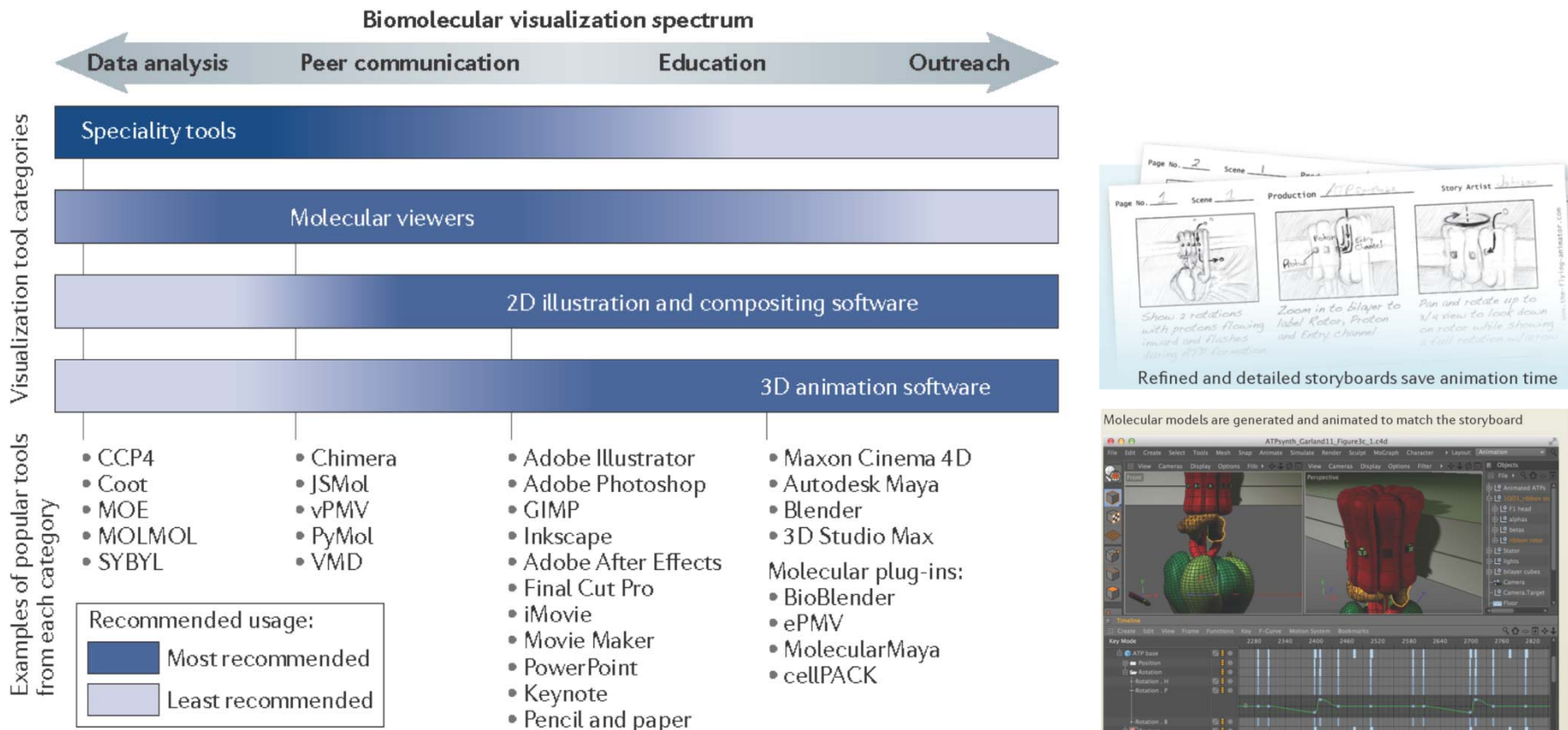
Schematic representation of the cryo-ET workflow



Lučić, V. et al. *JCB* (2014)



Biomolecular Visualization Tools



Johnson, G and Hertig, S. *Nat Rev Mol Cell Biol.* (2014) 10:690-8.





Acknowledgements

Juergen Plitzko
Friedrich Foerster
MPI of Biochemistry

Wolfgang Baumeister
MPI for Biochemistry

Present and former members
of the Structural Biology
at the MPI of
Biochemistry